AN ARCHITECTURAL INVESTIGATION OF WELL-DEFINED GRAFT COPOLYMERS BY CONTROLLED ACYCLIC DIENE METATHESIS (ADMET) POLYMERIZATIONS

By

PATRICK M. O'DONNELL

A DISSERTATION PRESENTED TO THE GRADUATE SCHOOL
OF THE UNIVERSITY OF FLORIDA IN PARTIAL FULFILLMENT
OF THE REQUIREMENTS FOR THE DEGREE OF
DOCTOR OF PHILOSOPHY

UNIVERSITY OF FLORIDA

2002

To my grandparents, Jack and Mildred, for their never ending love and support. They taught me how to be proud of who I am and what it takes to accomplish my dreams.

ACKNOWLEDGMENTS

My time in graduate school has been intellectually stimulating, rigorous, at times frustrating, but overall an enjoyable experience. As I have been told several times by my advisor Dr. Wagener, this is my time and only I can decide how to spend it. I am thankful for the freedom I have been given to explore, learn, fail, and to learn from my failures. However, there have been several individuals that have helped me along this path and it would not have been possible without them.

First, a special thanks to those past and present members of the Wagener research group, especially Dr. Krystyna Brzezinska, Dr. James Pawlow, Dr. Mark Watson, Dr. Debbie Tindall, Dr. Fernando Gomez, Dr. A. Cameron Church, Dr. Jason Smith, John "Shaggy" Schwendeman, Ed Lehman, John Sworen, Tim Hopkins, and Violeta Petkovska. All have been gracious about offering their help and insight, especially Krystyna. She was instrumental in the beginning of my graduate career and was always helpful and insightful in the lab. This group, and members of the polymer floor, have provided a learning experience that has been enjoyable and fulfilling. This type of atmosphere would not have been possible if it had not been for Dr. George B. Butler. His generosity to the chemistry department and polymer floor is greatly appreciated. I would also like to thank members of the Reynolds research group: Dr. Luis Madrigal, Dr. Dean Welsh, Dr. Michael Ramey, Carl Guapp and Irina Schwendeman, for their support as well. We have all spent so much time together in and outside of lab, I am truly grateful for all the friendships that have come along with the learning.

I also want to acknowledge my parents John and Barbara O'Donnell for their support and love. They know what I have gone through more than anyone else. It was not always an easy time over the past few years, but they have always believed in me and supported my choices as parents do.

I would also like to thank my roommates and friends that I have encountered during my time here. They were always great and have provided me with memories that I will never forget. Joe McClellan and James "Murf" Murphy were always there to remind me that they were Holy Cross graduates, and I was not. Of course, Murf has been much more than this, and that is what I will always appreciate. Shaggy was great at keeping us on our toes, we never knew what to expect next and I do not think he did either. Olivia Bautista has been a rock of support and I know that I will always be able to count on her. I am also grateful for the friendship of Leonard and Becky Rorrer, especially during the last year. I would also like to thank Dawn Bradly for her special friendship and help in preparing this document. All of these people, and many others, have made my time at UF a fulfilling and unique experience.

Thanks go to the members of my committee: Dr. John Reynolds, Dr. Eric Enholm, Dr. Jon Stewart, and Dr. Chris Batich. I would also like to thank Dr. David Powell for his assistance with the MALDI-TOF, and Dr. Ion Ghivirga for providing excellent NMR facilities. I also need to thank Mrs. Lorraine Williams for her kindness and gracious assistance in the polymer office during more times than I can count. It is a wonder how well she balances everything with such ease. I would also like to thank Ms. Donna Balkom and Ms. Lori Clark for their time and effort in the graduate office.

I am also grateful for the support of my advisor Dr. Kenneth B. Wagener. He always believed in my efforts and never let me give up. Without his endless support, freedom and generosity, none of this would have been possible.

Finally, I would like to extend my gratitude to the National Science Foundation and the University of Florida for their financial support of my graduate career.

TABLE OF CONTENTS

page

LIST OF TABLES

LIST OF FIGURES

Abstract of Dissertation Presented to the Graduate School
of the University of Florida in Partial Fulfillment of the
Requirements for the Degree of Doctor of Philosophy

AN ARCHITECTURAL INVESTIGATION OF WELL-DEFINED GRAFT COPOLYMERS BY CONTROLLED ACYCLIC DIENE METATHESIS (ADMET) POLYMERIZATIONS

By

Patrick M. O'Donnell

August 2002

Chair: Professor Kenneth B. Wagener
Department: Chemistry

By taking advantage of the well-defined Acyclic Diene Metathesis (ADMET) polymerization mechanism, new synthetic methods have been developed in order to acquire a controlled molecular design. By combining the macromonomer technique with ADMET, precise graft copolymer architectures have been achieved. These comb structures are a direct result of proper monomer design prior to metathesis polymerization.

Several structural variables have been optimized in order to control the physical nature of the resulting macromolecules. Features such as placement and concentration of the graft site along the polyolefin backbone, chemical nature of the graft, and length and polydispersity of the graft. These modifications have been achieved through "living" techniques by ionic polymerizations or Atom Transfer Radical Polymerizations (ATRP). These techniques have allowed for the functionalization of several polymers such as

polystyrene, poly(methyl methacrylate) and poly(ethylene oxide) with an α,ω-diene ADMET precursor. Thus, the metathesis polycondensation results in a combination of two different homopolymers.

The resulting covalent bonds beween the two homopolymers lead to interesting thermal investigations. As a result of the chemical linkage, the properties were unlike either the homopolymers or a random copolymer blend. These results are an indication of the regularity attainable by the ADMET mechanism which are not readily possible by other typical polymerization methods.

CHAPTER 1
INTRODUCTION

The design and synthesis of polymeric materials has developed into a useful and essential area of modern chemistry. Polymer science examines the demand for everyday challenges requiring the use of efficient polymerization techniques. However, such techniques require that viable routes toward specific structures are constantly being developed and explored in order to further the advancement of the field. The fact that this area of science can yield materials with designed genuine properties exhibits the progress brought fourth by molecular architectural engineering.

The dissertation will focus on the development of new polymeric materials and their unique properties based upon a more tightly controlled macromolecular structure. The work presented is based upon the fundamentals of polymer chemistry in order to control the outcome of the physical properties. This control over the microstructure will be demonstrated through the behavior of the resulting material. By designing several copolymer systems through a variation of monomers and mechanisms, a modern polymer chemist can design several macromolecular structures with a variation of results.

Copolymers

By convention, a copolymer is defined as a product between two monomers in which each is capable of forming a homopolymer under the appropriate conditions. The outcome of these copolymers leads to a macromolecule in which the properties are different from either homopolymer due to the chemical linkage between the two

monomers. Within this definition of a copolymer are several different classifications developed by Ceresa in 1961 based upon spatial arrangement and architectural design of the final product such as random, alternating, block, segmented, and graft copolymers.

Random and Alternating Copolymers

Random copolymers are the most common type of copolymer (Figure 1-1). They are the most versatile, economical, and easily synthesized copolymer; and characterization is based upon statistical placement of the comonomer repeat units. The polymer can be synthesized through free radical, ionic addition, ring-opening polymerization, and step-growth polymerization methods.

Figure 1-1. Random copolymers.

Alternating copolymers are typically formed through a chain reaction in which one monomer unit adds onto a second monomer unit in a strict manner (Figure 1-2). Alternating copolymers are typically rare systems due to strict reaction conditions and are fovorable either through a pair of monomers with highly specific copolymerization reactivity ratios and/or special conditions.

Figure 1-2. Alternating copolymers.

The incentive to synthesize such systems is the achievement of a homogenous system that displays properties of the weighted average of the two repeat units. However, it is

the random copolymers that closely approximate this situation and allow for this average of physical properties (Tobolsky 1960).

Block Copolymers

Block copolymers are comprised of chemically dissimilar, terminally connected segments (Noshay and McGrath 1977). As shown in Figure 1-3, their arrangement can vary from two segments with A-B block copolymers or three segments with A-B-A block copolymers. In addition, segmented block copolymers have a repeat unit, $(A\text{-}B)_n$ to yield a multiblock system. Essentially, block copolymers have fewer and longer chains, and segmented copolymers have a greater number of shorter chains along the polymer backbone.

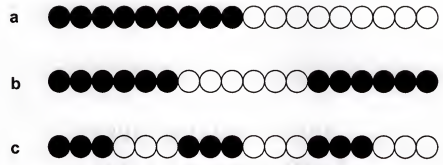

Figure 1-3. Block copolymers (a) A-B block copolymers, (b) A-B-A block copolymers, (c) Segmented block copolymers.

Several synthetic methods are used to synthesize these architectures including step-growth, anionic, cationic, and free radical polymerizations (Morton and Fetters 1967, Szwarc 1968, Hoffman and Bacskai 1964). However, the best copolymer techniques are based upon sequential anionic addition or ring-opening polymerization due to consecutive addition of the monomer which is important for obtaining the ultimate properties. There is a high degree of difficulty associated with the synthesis of these

structures because of the requirements imposed on these systems. These polymerizations require an accurate knowledge and control of initiating and propagating species, low impurity levels, the use of low concentration solution polymerization methods, and the need for separately producing reactive polymeric intermediates of known functionality.

Graft Copolymers

Graft copolymers, as defined by Battaerd (Battaerd and Tregear 1967), are molecules that are comprised of two or more polymeric parts of different compositions in which one type of polymer has subsequent polymerization of another kind of polymer along the backbone (Figure 1-4). The presence of this chemical bond between two homopolymers has a significant impact on the physical properties and as a result graft copolymers are strikingly similar to block copolymers.

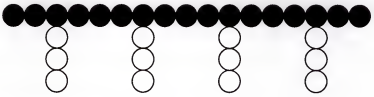

Figure 1-4. Graft copolymer architecture.

Graft copolymers are generally prepared through step-growth, free radical, anionic, cationic, or ring-opening polymerizations in the presence of a preformed reactive polymer. Typically, step-growth polymerizations are not highly considered due to their di- or multi-functional nature that which allows for cross-linked systems to occur. Therefore, commercial graft copolymers are prepared through free radical polymerizations.

The first category of free radical polymerizations involves the polymerization of an olefinic monomer in the presence of a preformed polymer bearing a labile hydrogen.

Initiation occurs through typical methods followed by abstraction of the labile hydrogen. Then, the initiator or growing chain produces radicals on the polymer backbone through the labile hydrogen. The link between the graft and the backbone can be formed via monomer initiation by the backbone radical or by recombination reactions. Fischer (1973) was able to accomplish this by grafting styrene onto polybutadienes.

Another category of preparing graft copolymers through free radical initiators is hydroperoxidation (Battaerd and Tregear 1967). The monomer is initiated by hydroperoxide or functional groups already on the preformed polymer backbone. Even though these are powerful techniques for commercial applications, they are still characterized with broad compositional heterogeneity and contaminated with homopolymers. A better control of the structure with less homopolymer contamination can be gained through anionic methods which lower the propensity for spontaneous termination (Kennedy et al. 1974).

All of the previous synthetic methods involve grafting from an initiator along a multifunctional polymeric precursor. In addition to the "grafting from" technique, other strategies are available for the synthesis of graft copolymers. Jerome (1999) has discussed "grafting onto" and "macromonomer" techniques. "Grafting onto" is the coupling of functional polymers with mutually reactive groups on each homopolymer. The macromonomer technique places the graft in the monomer prior to the copolymerization which allows for a wide variety of macro- and co-monomers. However, the extent of the reaction is often limited by the branch character and ill-defined architectures as a result of radical initiation. The macromonomer approach of graft copolymers will be discussed later.

Due to the complex and intricate design of graft copolymer architectures, complete characterization is often a difficult task. In the case of linear homopolymers, ideally only the length of the molecule will vary, but block and graft copolymers can also vary in length, composition, and structure. While the number of segments in a block copolymer can be deduced with some degree of certainty from synthetic techniques, the same cannot always be determined for graft copolymers due to their multifunctional nature. The efficiency to which these functionalities participate must be questioned; in addition, the length and polydispersity of the grafts must be considered.

Since a graft copolymer is a combination of different homopolymers, it is commonly considered as a hybrid molecule. Even though it is a single chemical species, the behavior of this molecule can display the properties of both components rather than an average. Graft copolymers are often insoluble in the solvents of either corresponding homopolymeric material. When examining thermal behaviors, a single-phase morphology is possible, but a two-phase morphology is much more commonly observed (Stannett 1977). Typical transitional thermal behaviors display two distinct glass transition temperatures and/or melt transition temperatures. However, due to intersegmented linkages, they display a finer morphology depending upon the chemical matrix. Thus, at times an amorphous system would show good optical clarity in the absence of homopolymer contamination. Yet, it is also possible to blend a two-phase graft copolymer with their homopolymer. This feature has a utility whether the components are rigid or elastomeric.

This dissertation will further discuss synthetic methods utilized to obtain such a macromolecular design and the manner in which they were characterized.

Olefin Metathesis

The history of olefin metathesis chemistry dates back to over 50 years ago with the advent of Ziegler-Natta transition metal catalysts for olefin polymerization (Crabtree 1994). In turn, it has developed into a useful modern synthetic tool of specialty polymers, fine chemicals, natural products which continues to be developed for several other applications.

Essentially, olefin metathesis is an equilibrium process in which there is the exchange of carbon moieties between a pair of double bonds in two alkene molecules (Figure 1-5).

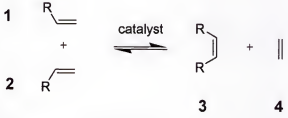

Figure 1-5. Olefin metathesis of a terminal alkene.

However, the true mechanism pathway was not always easily understood. From the mid-1950s to early 80s, olefin metathesis was performed with ill-defined, multi-component, homogenous and heterogeneous catalyst systems. Such catalyst systems for the polymerizations of olefins often involved the in situ formation of the catalyst. Some of these classical combinations include WCl_6/Bu_4Sn, $WOCl_4/EtAlCl_2$, MoO_3/SiO_2, and Re_2O_7/Al_2O_3. These particular ill-defined systems were complex and often difficult to understand. Even though the exact nature of the mechanism was not yet understood during this time, olefin metathesis developed into a powerful organic tool for the transformation of diene monomers to high molecular weight polymers. Eventually, Chauvin proposed a mechanism involving the interconversion of a metal alkylidene (**5**)

and an olefin (**6**) in which olefin containing compounds were divided at the carbon-carbon bond into carbene fragments and then redistributed into new olefins (Herrison and Chauvin 1970). The key step in this mechanism was the formation of the metallobutacycle (**7**), which was formed by the interaction of a metal carbene with an olefin (Figure 1-6). The formation of this key intermediate resembles a [2+2] cycloaddition from which the olefin coordinates with the alkylidene. Cleavage of the ring can occur in either a vertical or horizontal manner. However, the productive cleavage of the metallacycle generates a new alkylidene (**8**) that is reactive upon exposure to a second olefin. Stereoselectivity of these systems are mainly determined by steric interactions between the ligand set of the alkylidene and the olefin substituents.

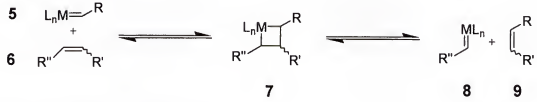

Figure 1-6. Metallobutacyle cleavage.

It has been noted by Ivin and Mol (1997) that two other factors must be considered as part of this mechanism: the equilibrium of every step, and the formation of the metallobutacycle intermediate and it's consideration as the rate determining step. Although the formation of this intermediate was first highly debated, it is now widely accepted as part of the mechanism in the scientific community.

With regard to the Chauvin mechanism, olefin metathesis can be categorized into several types of mechanisms depending upon the structure of the starting material.

However, it should be noted that each case entails both the metal carbene and the metallobutacycle intermediate.

Exchange Metathesis

Exchange metathesis (Figure 1-5) is the most simplified version of olefin metathesis. In this example, two molecules of a terminal (monosubstituted) olefin react to yield a disubstituted olefin (**3**) and a molecule of ethylene (**4**) as the by-product. This reaction proceeds with relative ease due to the low steric constraints of the molecule. In addition, since the second product of the reaction is ethylene, the equilibrium of the reaction can be driven to completion following Le Chatelier's principle. Removal or addition of any of the reactants or products may shift the equilibrium of the reaction. The stereochemical outcome is typically determined by the use of a particular catalyst in which geometry and ligand size constitute the outcome and the extent of the isomerization process.

Exchange metathesis can also occur between two similar or distinct disubstituted olefins, in which case cross metathesis takes place. Depending upon the nature of the starting materials and the known fact that this is a cis:trans equilibration the outcome of the reaction could be several different stereoisomers via repetitive degenerate metathesis. This event often hinders the use of this reaction as a synthetic tool; however, research in this field is still under investigation (Cossy et al. 2001).

Ring Closing Metathesis

Ring closing metathesis (RCM) has been extensively explored and reviewed by Grubbs (Grubbs and Chang 1998, Trnka and Grubbs 2001), and Wright (1999) for the synthesis of small molecules that are not attainable by conventional synthetic methods. This reaction consists of two tethered terminal olefins (**10**) reacting to yield a cyclic structure (**12**) as described in Figure 1-7.

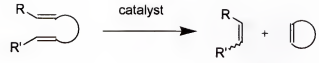

10 **11** **12**

Figure 1-7. Ring Closing Metathesis.

There are several components of RCM that allow this process to occur. First, the reaction is run in highly dilute conditions rather than bulk conditions in order to favor the intramolecular ring closure over a intermolecular reaction. Since these molecules are similar to those used in acyclic diene metathesis (ADMET), competition between both pathways does exist. In addition to concentration, chemical characteristics of the molecule must be taken into consideration to determine if RCM is feasible. The transformation to the metallacycle must consider thermodynamic and kinetic factors, such as intramolecular hydrogen bonding, ring strain (favorable ring size), and effect of the substituents. Bulky substituents in close proximity to the olefins also promote ring closing by the Thorpe-Ingold effect. Each variable is significant in determining the final product.

Ring Opening Metathesis Polymerization

In ring opening metathesis polymerizations (ROMP), cyclic olefins are converted to high molecular weight polymers under favorable thermodynamic conditions due to the release of ring strain (Figure 1-8). Even though ROMP is considered to be an equilibria reaction in theory, it is typically an irreversible process because of the highly favored thermodynamics of the system that allows the reaction to proceed in a rapid and exothermic manner. The strained olefins favor this process for rings of 3-, 4-, 8- and

larger-sized rings. However, in the case of cyclohexene, the stability of the 6-membered ring does not allow the equilibrium reaction to proceed as readily.

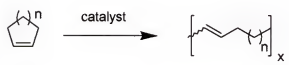

13 **14**

Figure 1-8. Ring Opening Metathesis Polymerization.

The ROMP mechanism is similar to ADMET, and several of the intermediates are analogous to ADMET intermediates. Both mechanisms proceed through the metallobutacycle, followed by ring cleavage to form the new linear, terminal carbene. Since the active center is attached to the chain end, the propagation step will continue the polymerization; thus, it should be noted that ROMP is a chain polymerization. However, due to a difference in driving forces and release of ring strain compared to removal of the condensate, ROMP is much faster than ADMET. Several reviews and discussions regarding ROMP have been published by Grubbs et al. (1997a, 1997b) and Schrock (1990, 1993).

Acyclic Diene Metathesis Polymerization

Acyclic diene metathesis (ADMET) polymerization is a step polycondensation to produce a linear, unsaturated hydrocarbon polymer. Terminal α,ω-dienes are connected via a stepwise manner to produce a polyolefin (**16**) and a molecule of ethylene (**17**) in each propagation step (Figure 1-9). Since the reaction occurs under equilibrium, this process is driven to completion by removal of the condensate. Therefore, by definition (Odian 1991), ADMET can be considered a step-propagation condensation-type polymerization.

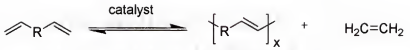

Figure 1-9. Acyclic Diene Metathesis Polymerization.

Recent reviews on ADMET have described the theory and experimental conditions (Tindall et al. 1998, Davidson and Wagener 1999, Church et al. 2002). ADMET has developed into a powerful tool for the synthesis of organic polymers. This mechanism allows for the synthesis of hydrocarbons and placement functionality within or along the polymer backbone simply through design of the monomer unit.

Since ADMET is an equilibrium reaction, the reverse reaction is a statistical possibility, in which the by-product may react with the main chain to form either smaller species, closed systems, and/or lower molecular weight products. However, it is also this equilibrium process that allows the reaction of all chains in the system to randomize the product distribution as described by the polydispersity (PDI = M_w/M_n) of 2.0. The process by which acyclic dienes are converted into unsaturated polymers is illustrated in Figure 1-10.

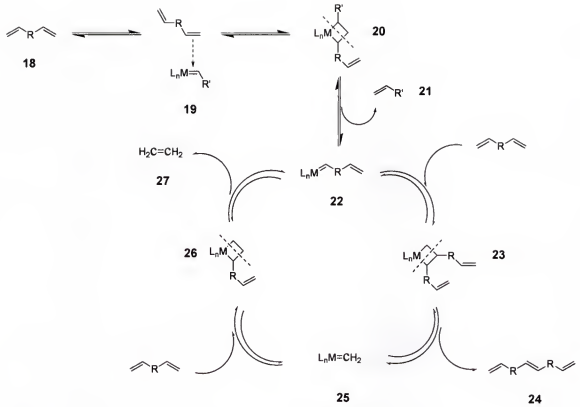

Figure 1-10. Acyclic Diene Metathesis (ADMET) mechanism.

The initiation step of the mechanism starts with the coordination of the metal alkylidene with a olefin site within the diene monomer (**18**). As a result, a π-complex (**19**) forms between the metal alkylidene and the olefin site, and eventually forms the metallabutacycle (**20**) previously discussed. The metallabutacycle then disproportionates to form a new alkene (**21**) while regenerating the alkylidene (**22**), placing the transition metal at the end of the propagating monomer chain. Another diene then interacts with the alkylidene as previously described to form a π-complex, rearranging into a metallabutacycle (**23**), which then disproportionates and condenses into the propagating polymer chain (**24**) in order to continue the cycle. Finally, ethylene (**27**) is the condensate of the reaction when α,ω-dienes are used in a step-growth polymerization.

Support of this mechanism and its second-order kinetics is well documented in the literature (Wagener et al. 1997a).

There are other factors that play a significant role in the mechanism. Sterics of the α,ω-diene monomer alkylidene are important factors in the kinetic rate of the mechanism. Depending upon the steric incumberance around the π-complexation, the rate of the reaction can be hindered or halted altogether. In addition, the presence of functionality can modify the reaction rates since electronics associated with the transition metal are attached to the propagating alkylidene chain. These factors will be left for a later discussion.

Polymer chemistry is classified into two basic categories based upon the propagating mechanisms of polymerization: chain and step propagation. In order to obtain a high degree of polymerization (X_n) for a typical step/condensation polymerization, the reaction must achieve 99.99% conversion before a high molecular weight polymer is formed. Monomer is consumed early in the reaction to form dimers, trimers, tetramers, etc. and the molecular weight is controlled by statistics associated with linking the ends of each monomer. Figure 1-11 displays a plot of the Carothers equation and illustrates the requirements of a step polymerization.

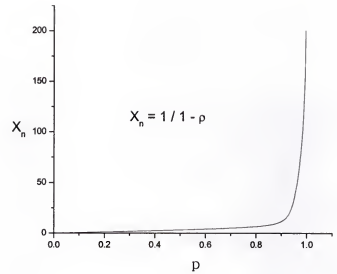

Figure 1-11. Plot of Carothers equation for a step polycondensation reaction.

As shown in Equation 1-1, the average degree of polymerization (X_n) is dependent upon extent of conversion (ρ) and stoichiometric imbalance ratio (r). When examining a step polymerization which only has one type of functional group, as for the ADMET acyclic diene monomers, then the stoichiometry is balanced and equation 1-1 is reduced to equation 1-2, the Carothers equation. Therefore in the case of ADMET, stoichimetric balance simply means that vinyl groups terminate all linear molecules in the system at both ends during the reaction.

$$Xn = \frac{1+r}{(1+r-2rp)}$$

Equation 1-1.

$$Xn = \frac{1}{1-p}$$

Equation 1-2.

Finally, the efficiency of a step polymerization is highly dependent upon monomer purity. Any type of contamination present during the metathesis reaction is detrimental to accomplishing a high molecular weight polymer.

Metathesis Catalysis

As previously discussed, the presence of a metal carbene is crucial to the metathesis reaction by forming the required metallobutacycle intermediate. A carbene is defined as an organometallic complex involving a metal-carbon double bond. The development of modern, well-defined catalysts was initiated in 1964 with Fischer carbenes (**28**), commonly known as carbenes, and expanded to Schrock carbenes (**29**), or alkylidenes, during the 1980's as seen in Figure 1-12. The fundamental difference between these two types of carbenes is Fischer carbenes show electrophilic behavior while Schrock carbenes exemplify nucleophilic behavior (Crabtree 1994, Elsenbroich and Salzer 1992).

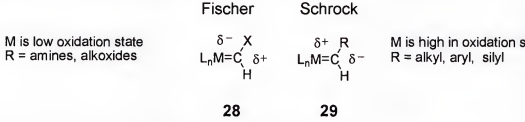

Figure 1-12. Structures of Fischer and Schrock carbenes.

Prior to these well-defined catalysts, olefin metathesis employed ill-defined systems (Ivin 1997). Even though these catalyst systems were useful, the mechanism was poorly understood due to their heterogeneous nature. Thus, it was for this reason that carbenes became employed for the metathesis mechanism (Herrison and Chauvin 1970).

Ill-Defined ADMET Catalysts

The first development of transition metal carbenes involved an in situ formation with a pre-catalyst and activator. These classical catalyst systems involved the formation of the carbene moiety during the reaction (Ivin 1997). Even though the mechanism of carbene formation is not well understood for these systems, it is known that they are efficient at elevated temperatures under ADMET conditions.

The first sucessful reports of ADMET polymerizations using WCl_6 and a tin activator were by Nubel et al. (1995). Since then, other classical catalyst systems based on aryloxide derivatives such as $WOCl_4$ and organotin activators have been reported to yield clean ADMET polymerizations (Gomez and Wagener 1998).

Well-Defined ADMET Catalysts

It was not until the advent of well-defined catalyst systems that the metathesis reaction became understood in a manner suitable for optimization conditions. It became apparent that proper catalyst choice is essential in order to avoid side reactions such as cation formation, vinyl addition, and the formation of multiple catalytic species (Wagener et al. 1990). The most common single site-catalyst/initiator systems for ADMET conditions typically require Schrock's carbene or Grubbs' alkylidene catalyst in order to proceed.

These catalysts offer the advantage of higher activities under milder conditions. By varying the ligand environment of the metal center, a tunable catalyst system can be developed. Also, by differing the steric and electronic nature of the alkoxide ligands, the reactivity of the metal alkylidene can be engineered to different degrees. However, these types of catalysts are also limited by their high oxophilicity of the metal centers which causes them to be highly sensitive to oxygen and moisture.

Schrock's catalyst systems were developed through variations of the ligand groups and metals with high oxidation states. Bulky imido and alkoxy ligands were attached to four coordinate W(VI) or Mo(VI) metal centers (Figure 1-13). Within these systems, various electronic and steric factors were accounted for while allowing the approach of the olefinic moiety. It was eventually realized that the highest degree of reactivity was accomplished when the alkoxy groups were hexafluoro-t-butoxy (Schaverien et al. 1986). Even though metathesis conditions were optimized in this manner, the W analogues **(30)**

would not tolerate any functionality. It was not until the development of the Mo analogues (**31**) that the catalyst became more tolerant of functionality. It was these Mo catalysts that allowed for ROMP and RCM substrates to include a broad range of functionalities (Schrock 1990). Eventually, these catalysts were developed to be suitable for ADMET, and the first report of Schrock's catalyst under ADMET conditions was reported in 1991 (Wagener et al. 1991). Even though the Schrock's catalyst systems were a significant achievement, they still were not tolerant of functionality within the polymer. In addition, they are highly unstable during storage and are sensitive to air and moisture and easily deactivated. It was not until the advancement of Grubbs' ruthenium based systems that some of these problems were overcome.

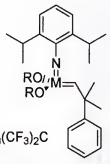

30 M = W
31 M = Mo

Figure 1-13. Schrock's carbene for olefin metathesis.

In the 1990s, ruthenium based catalysts were explored in order to compensate for the issue of functionality of the substrate or solvent binding to the metal center and deactivating the catalyst in the Schrock-type systems (Trnka and Grubbs 2001). Ruthenium was chosen because of its higher reactivity to olefins than any other transition metal system. Therefore, Grubbs developed robust, functional group tolerant, benzylidene catalyst systems. The first reports of discrete ruthenium carbene complexes

(**32**) were published in 1993 (Nguyen et al. 1993) and again later with significant improvements (**33**) in 1996 (Schwab et al. 1996) and most recently (**34**) in 1999 (Scholl et al. 1999). The development of these catalyst structures were a result of changing molecular features to acquire higher degrees of activity. There have also been several other publications over the years that have contributed to the development of ruthenium complexes such as Herrmann's (Herrmann et al. 1997, Weskamp et al. 1998 and 1999) and Nolan's (Huang et al. 1999) catalyst.

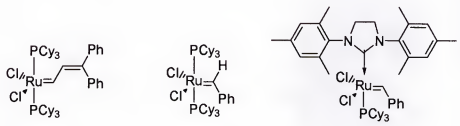

32 **33** **34**

Figure 1-14. Well-defined ruthenium carbenes for olefin metathesis.

These ruthenium catalyst systems are well-defined structures that are efficient under less stringent conditions. Although they are not as reactive as Schrock's alkylidenes, these catalysts can be handled in the presence of air while remaining active. The electronic properties of the ruthenium systems are different from Schrock's catalyst. The ruthenium is not in a high oxidation state, and the halogens have been included as electron withdrawing ligands. In addition, the phosphine ligands are excellent σ-donors. The sterics of these systems were constantly examined and fine-tuned to identify the affects of ligand structure.

The initial ruthenium complex (**32**) was not as reactive as Schrock's Mo catalyst, but it was the first well-defined complex tolerant of functionality due to high stability with

respect to the vinylidene benzylidene. It is a very robust catalyst that is air-stable as a solid and retains activity when exposed to water, alcohols, or acids. Upon combining bulky and strong electron donating PCy_3 ligands, the activity of the benzylidene ruthenium catalyst (**33**) was greatly increased. The benzylidene catalyst became the preferred form of the alkylidene because of the ease of synthetic preparation.

Both types of well-defined catalyts have proven to be useful in ADMET polymerizations for unique and specific monomer properties. The Schrock's systems have greater activities due to faster polymerization kinetics. However, systems such as Grubbs' carbenes have proven to be more versatile and enduring for systems with polar functionalities.

Functional ADMET Polymers

Monomer design has proven to be fundamental when the placement of functionality is incorporated into ADMET polymers. Essentially, any terminal diene can be polymerized using ADMET chemistry. However, the transition metal catalyst systems used are inherently Lewis-acidic. Thus, any acid-base interaction could possibly deactivate the catalyst. Therefore, the use of functionality within the monomer during a polymerization creates a fine balance of experimental conditions.

In addition to the electronics of the system, sterics play an important role in what is known as the *negative neighboring effect* (Wagener 1997a). This effect describes the differences in monomer reactivities with a discrepancy between the methylene spacing units. Some of the functional ADMET polymers displayed in Figure 1-15 include several oxygenated functionalities such as polyesters, polyethers, polyalcohols, polysiloxanes, and polyamino acids.

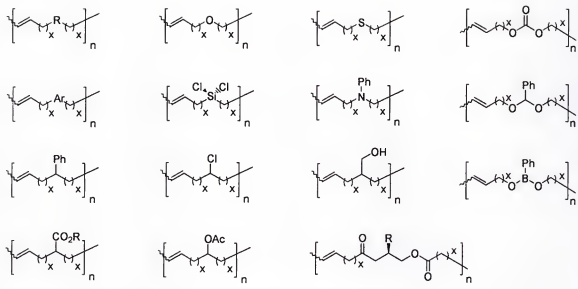

Figure 1-15. Functional ADMET polymers synthesized to date.

This integration of heteroatoms along and within the polymer backbone has allowed for the development of various materials through efficient means. These synthetic methods have been instumental in the development of several polymer structures that would not have been possible by conventional polymerization methods.

ADMET Architectures

Monomer design is crucial when considering the architecture of ADMET polymers. Physical properties and applications of the resulting polymer are often a consequence the of composition and tertiary structure of the polymer. By further exploring macromolecular architectures and their properties, one can develop predictable behavior through reasonable model studies.

Perfectly linear polymers can be synthesized by ADMET simply by homopolymerizing 1,9-decadiene to yield linear polyethylene. The mechanism of the reaction does not allow for any other side products such as branch content. However, by modifying the structural composition of the monomer, vastly different properties can result. Modeling polyolefin crystallization behavior using ADMET chemistry is an area

of extensive research. The polymerization of symmetrical α,ω-dienes containing an alkyl substituent (i.e. methyl, ethyl, hexyl, gem-dimethyl) and its subsequent hydrogenation yields polyethylene with a highly defined branch content (Smith 2000 et al., Schwendeman and Wagener 2002a). This methodology is significant due to its mimicking behavior of ethylene randomly copolymerizing with propylene.

In addition to linear polymers, several types of copolymer architectures are possible through step-polycondensation chemistry. Among these structures, segmented copolymers have been attained through ADMET polymerizations (Figure 1-16). These types of materials have been synthesized through the design of diene-terminated oligomers (diene telechelomers) that can be homo- or copolymerized with other terminal dienes. These telechelomers can exhibit properties such as phase separation, ampiphilic behavior, or increased blend compatibility. They have been incorporated as the soft phase in copolymers with hard polyalkenylene, polyester and polyurethane segments (Wagener et al. 1997b, Tindall et al. 1999).

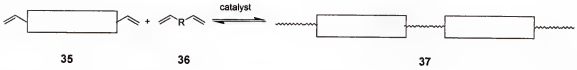

Figure 1-16. Segmented copolymers through ADMET polymerizations.

Other notable applications of telechelic polymers by end functionalized oligomers include polyalkenylenes created through the addition of a chain limiter (Figure 1-17). ABA triblock copolymers have been synthesized in which chlorosilane- and methoxysilane-terminated polyoctenylene have been copolymerized with hydroxyl-terminated silicones (Brzezinska et al. 1999). In addition, this same type of method has

been utilized to synthesize amorphous telechelic hydrocarbon diols with precise gem-dimethyl substitution occurring regularly along the polymer backbone (Schwendeman and Wagener 2002b).

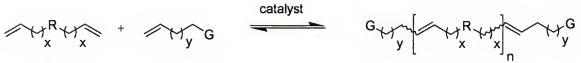

38 **39** **40**

Figure 1-17. End-functionalized ADMET telechelic polymers.

Finally, the use of functionalized α,ω-dienes has shown to be an effective tool for precursors to ADMET graft copolymers (O'Donnell et al. 2001). Typical polymerization methods make it nearly impossible to achieve complete regularity of these types of architectures (Burchard 1999). Imperfections in the spacing and length of the graft are typical of the chemical synthesis. Yet it is the metathesis mechanism that allows for complete regularity along the polymer backbone.

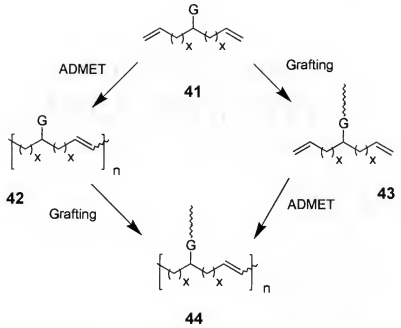

Figure 1-18. Graft copolymers via macroinitiator and macromonomer pathways.

These structures can be acquired through two separate mechanisms defined as the "grafting from" and "macromonomer" techniques (Jerome 1999). The "grafting from" approach allows the diene (**41**) to initially undergo metathesis followed by grafting of the polymer backbone (**42**). The "macromonomer" method grafts the copolymer to the functional site (**43**) prior to metathesis polymerization to ensure regular grafting along the polymer backbone (Figure 1-18). The final composition and architectural properties of the polymer are determined by several factors such as nature of graft, density of the graft along the polymer backbone, length of the graft and structure of the macromonomer.

CHAPTER 2
EXPERIMENTAL

Instrumentation and Analysis

^1H NMR (300 MHz) and ^{13}C NMR (75 MHz) were obtained and recorded on a Gemini Series NMR Superconducting spectrometer system or a Varian VXR-300. ^1H and ^{13}C NMR chemical shifts were referenced to original signals from chloroform-d ($CDCl_3$) with 0.05% TMS internal reference, dimethyl sulfoxide-d_6, or benzene-d_6 (C_6D_6). Gas chromatography (GC) was conducted on a 17A Shimadzu GC-17 gas chromatogram equipped with 15m or 25m a silica capillary and flame ionization detector. Low and high-resolution mass spectrometry (LRMS and HRMS) data were acquired on a Finnegan MAT 95Q hybrid section mass spectrometer using either electron or chemical ionization. Matrix-assisted laser desorption/ionization (MALDI) mass spectra were obtained on a Bruker Reflex II. For MALDI spectra data, *all-trans*-retinoic acid was used as matrix material for polyether samples, dithranol was employed as the matrix for polystyrene samples, and $CuCl_2$ used as the cationization reagent in a THF solution. Elemental analyses were conducted by Atlantic Microlabs, Inc., Norcross, GA.

Gel permeation chromatography (GPC) was performed using a Waters Associates Liquid Chromatograph U6K equipped with a SD-300 Dynamax pump, TC-45 Eppendorf column heater set at 35°C, and tandem ABI Spectraflow 757 UV absorbance/Hewlett Packard 1047-A refractive index detectors. The GPC solvent delivery system was configured for elution with either HPLC grade $CHCl_3$ or certified THF. Polymer samples were prepared in certified $CHCl_3$ or THF (~5 mg/mL) and slowly passed through a 0.45

μm syringe filter prior to injection. Samples were injected at a flow rate of 1.0 mL/min into a cross-linked column of polystyrene divinylbenzene bed from American Polymer Standards. Retention times were calibrated against narrow (polydispersity < 1.13) polystyrene standards from Polymer Labs with M_p = 580, 1260, 2350, 5000, 10 050, 21 000, 38 100, 65 500, 151 700, 275 200 g/mol.

Differential scanning calorimetric (DSC) and thermogravimetric analysis (TGA) data were obtained using a Perkin Elmer DSC 7 equipped with a controlled cooling accessory (CCA-7) at a heating rate of 10°C/min. DSC samples (5-10 mg) were dried at 40-50°C for 24 hr at 0.1 mm Hg under reduced pressure prior to analysis. Helium (alumina column dried) was used as the carrier gas due to the extreme subambient temperatures involved. Instrument calibration was accomplished using ultrapure *n*-octane, indium, and/or zinc as standards for peak temperature transitions, and indium for the enthalpy standard. After an initial scan, samples were heated 40°C above the melting point, if observed, to erase the thermal history before undergoing further scans. Samples were then cooled to approximately 30°C below the initial thermal transition and heated to approximatley 40°C above the the highest thermal transition. Data was collected on the second or third scan until constant thermal behavior was observed.

Materials and Techniques

Grubbs' first generation benzyidene catalyst, $[Ru(=CHR)(PCy_3)_2Cl_2]$ and second generation catalyst $[Ru(=CHR)(SIMes)(PCy_3)Cl_2]$ where Cy = cyclohexyl and R = phenyl, were prepared according to literature procedures (Nguyen et al. 1993). A 1.0 M solution of tris(hydroxymethyl) phosphine in isopropanol (THP) was obtained from Materia (Pasadena, CA). Tetrahydrofuran (THF), 1,2-dimethoxyethane (DME), and

diethyl ether, were dried over CaH_2 and further distilled under argon from Na/K alloy prior to use and stored over 5 A molecular sieves. Toluene was washed with cold concentrated H_2SO_4, dried with $MgSO_4$, CaH_2 and further distilled under argon from Na/K alloy and stored over 5 A molecular sieves. Ethyl acetoacetate (Aldrich), methoxy ethoxy methyl chloride (Aldrich), 1,9-decadiene (Aldrich), 5-bromo-pentene (Aldrich), 11-bromo-undecene (Fluorochem), and propylene oxide (Aldrich) were stirred over CaH_2 and vacuum transferred prior to use. Potassium *tert*-butoxide (KOt-Bu) (Avacado) was dried under vacuum at 60°C for 24 hr in a flame dried, argon purged schlenk tube. A solution of 2M KOt-Bu was prepared by adding DME freshly distilled from a Na/K alloy. Naphthalene (Aldrich) was recrystallized in MeOH and added to sodium metal in freshly distilled THF to prepare a 0.3 M solution of potassium naphthalide. Diphenyl ether (Aldrich) was recrystallized in 95% MeOH, melted, dried over $CaCl_2$ and fractionally distilled prior to use. Styrene (Aldrich) was washed with $NaHCO_3$ and deionized water to remove inhibitors and distilled over CaH_2 at reduced pressure. Ethylene oxide (Aldrich) was condensed over CaH_2 at –78°C for 2 hr, and further dried over *n*-BuLi for 30 min prior to use (CAUTION: ethylene oxide is a highly volatile and poisonious gas). Denatured/anhydrous ethanol (Aldrich), 21% (w/w) sodium ethoxide (Aldrich), 1.0 M lithium aluminum hydride in diethyl ether (Aldrich), 1.6 M *n*-BuLi in THF (Aldrich), tetrafluoroboric acid-diethyl ether complex (Aldrich), 1-bromo-2,2-dimethyl propionic acid (Aldrich), 4-dimethylaminopyridine (Acros), 1,3-dicyclohexylcarbodiimide (Aldich), 1-(3-dimethylaminopropyl)-3-ethylcarbodiimide hydrocholride (Aldrich), copper (I) bromide (Aldrich), and 2,2'-bipyridine (Strem) were used without further purification.

Synthesis and Characterization

Synthesis of Poly(ethylene oxide) Based Macromonomers

Dialkylation of Ethyl Acetoacetate. Synthesis of ethyl-2-acetyl-2-(4-pentenyl)-6-heptenoate (**3.4**). Ethyl acetoacetate (10.9 g, 84 mmol) was added to 200 mL of 1,2-dimethoxythane in a flame-dried, argon purged 500 mL 3-neck flask equipped with a stir bar and condenser. A 42 mL portion of 2M potassium *tert*-butoxide solution was added via syringe and stirred at room temperature for 30 min. The solution was cooled to 0°C and one equivalent of 5-bromo-pentene (12.5 g, 84 mmol) was added via syringe over 5-6 min. The reaction was slowly brought to reflux and allowed to stir for 18 hr. The mixture then became orange-brown in color. The solution was then cooled to room temperature and a second equivalent of potassium *tert*-butoxide (42 mL, 1.0 M solution) and 5-bromopentene (12.5 g, 84 mmol) were added in the same manner as above. The solution was brought to reflux and stirred for an additional 26 hr. The reaction mixture was cooled to room temperature, and quenched with 3N HCl, washed with 3 times with deionized water, and extracted three times with Et_2O. All organics were combined and subsequently dried with anhydrous $MgSO_4$, filtered, and concentrated under reduced pressure to yield a yellow liquid product. Crude yield: 94.6%. Spectral properties observed: ^{1}H NMR ($CDCl_3$): δ 1.09 (m, 4H), 1.19 (t, 3H), 1.78 (m, 4H), 2.05 (q, 4H), 2.11 (s, 3H), 4.11 (q, 2H), 4.89 (m, 4H), 5.65 (m, 2H). ^{13}C NMR ($CDCl_3$): δ 13.91, 23.01, 26.46, 30.54, 33.41, 60.94, 63.17, 114.93, 137.78, 172.34, 204.98. Full characterization described earlier (Valenti 1998).

Synthesis of 2-acetyl-2-undec-10-enyl-tridec-12-enoic acid ethyl ester (**3.5**). Ethyl acetoacetate (7.0 g, 54 mmol) was added to 200 mL of 1,2-dimethoxythane in a flame-

dried, argon purged 500 mL 3-neck flask equipped with a stir bar and condenser. A 27 mL portion of 2M potassium *tert*-butoxide solution was added via syringe and stirred at room temperature for 30 min. The solution was then cooled to 0°C and the first equivalent of 11-bromo-1-undecene (12.5 g, 54 mmol) was added via syringe over 5-6 min. The reaction was slowly brought to reflux and allowed to stir for 24 hr. The mixture then became canary-yellow in color. The solution was cooled to room temperature and the second equivalent of potassium t-butoxide (27 mL, 1.0 M solution) and 11-bromo-1-undecene (12.5 g, 54 mmol) was added in the same manner as above. The mixture was then brought to reflux and stirred for an additional 36 hr. The mixture was cooled to room temperature, and quenched with 3N HCl, washed 3 times with deioinized water, and extracted 3 times with Et_2O. All organics were combined and subsequently dried with anhydrous $MgSO_4$, filtered and concentrated under reduced pressure to yield a yellow liquid product. Crude yield: 95.3%. Spectral properties observed: ^{1}H NMR ($CDCl_3$): δ 1.14 (m, 42H), 1.74 (m, 4H), 1.95 (q, 4H), 2.01(s, 3H), 4.08 (q, 2H), 4.88 (m, 4H), 5.71 (m, 2H). ^{13}C NMR ($CDCl_3$): δ 13.92, 23.71, 26.45, 27.26, 28.82, 28.96, 29.29, 29.39, 29.92, 31.36, 33.60, 45.55, 59.85, 60.75, 63.46, 71.76, 113.96, 138.90, 172.53, 204.89. Full characterization described earlier (Smith 2000).

Retro-Claisen Condensation. Synthesis of ethyl-2-(4-penteyl)-hept-6-en-oate (**3.6**). To a flame-dried, argon purged 250 mL 3-neck flask equipped with stir bar and condenser, the disubstituted β-keto-ester **3.4** (16.31 g, 61.3 mmol) was dissolved in 100 mL of denatured/anhydrous ethanol. The 21% (w/w) NaOEt/EtOH solution (22.12 g, 325.0 mmol) was then added slowly via syringe. This mixture was heated to reflux and stirred for 10 hr. After cooling the mixture the reaction vessel to room temperature, the

reaction mixtue was quenched with 3N HCl, washed 3 times with deionized water, and extracted 3 times with Et_2O. The combined organics were dried with anhydrous $MgSO_4$, filtered, and concentrated under reduced pressure. The crude product was placed into a vigerux distillation apparatus with CaH_2 and stirred overnight under vacuum. The crude product was then distilled and collected at 76-80°C with < 1.0 mm Hg as a colorless liquid. Isolated yield: 64.4%. Spectral properties observed: ^{1}H NMR ($CDCl_3$): δ 1.23 (t, 3H), 1.42 (m, 6H), 1.58 (m, 2H), 2.03 (q, 4H), 2.36 (m, 1H), 4.17 (q, 2H), 4.96 (m, 4H), 5.76 (m, 2H). ^{13}C NMR ($CDCl_3$): δ 14.36, 26.68, 31.93, 33.62, 45.47, 60.03, 114.65, 138.49, 176.28. Full characterization described earlier (Valenti 1998).

Synthesis of 2-undec-10-enyl-tridec-12-enoic acid ethyl ester (**3.7**). To a flame-dried, argon purged 250 mL 3-neck flask equipped with stir bar and condenser, the disubstituted β-keto-ester **3.5** (21.64 g, 51.1 mmol) was dissolved in 100 mL of anhydrous ethanol. The 21% (w/w) NaOEt/EtOH solution (18.42 g, 270.7 mmol) was added slowly via syringe. The mixture was heated to reflux and stirred for 10 hr. After cooling the reaction vessel to room temperature, the reaction mixture was quenched with 3N HCl, washed 3 times with deionized water, and extracted 3 times with Et_2O. All combined organics were dried with anhydrous $MgSO_4$, filtered, and concentrated under reduced pressure. The crude product was placed into a vigereux distillation apparatus with CaH_2 and stirred overnight under vacuum. The crude product was dried over CaH_2 and distilled at 0.1 mm Hg and collected at 175-180°C as a colorless liquid. Isolated yield: 48.3%. Spectral properties observed: ^{1}H NMR ($CDCl_3$): δ 1.34 (m, 38H), 1.56 (q, 4H), 2.01 (q, 4H), 2.27 (m, 1H), 4.09 (q, 2H), 4.98, (m, 4H), 5.76 (m, 2H). ^{13}C NMR ($CDCl_3$): δ 14.31, 27.38, 28.93, 29.08, 29.51, 29.69, 32.46, 33.73, 45.74, 59.81, 114.04, 139.17,

177.01. EI/HRMS: FAB calc'd for $C_{26}H_{49}O_2$: 393.37, found: 393.37. Anal calc'd for $C_{26}H_{49}O_2$: 79.59 C, 12.24 H; found 79.44 C, 12.38 H.

Ester Reduction to the Alcohol. Synthesis of 2-(4-pentenyl)-hept-6-en-1-ol (**3.8**). To a flame-dried, argon purged 500 mL 3-neck flask equipped with a stir bar, the pure ester **3.6** (11.46 g, 51.2 mmol) was dissolved in 200-225 mL Et_2O. The solution was cooled to 0^oC and 1.0 M LAH/Et_2O solution (102 mL) was added slowly via syringe. The reaction was then warmed to room temperature and stirred for 6 hr. The reaction was then transferred to a large beaker and the LAH was quenched slowly with deionized water (dropwise addition) under an argon atmosphere. After formation of an unstirrable gel, quenching was completed with 3N HCl. The resultant mixture was extracted 3 times with Et_2O and dried over anhydrous $MgSO_4$, filtered, and concentrated under reduced pressure. The crude product was dried over CaH_2 and stirred overnight under vacuum. The crude alcohol was then distilled and collected at 82-85°C under a vacuum of 0.1 mm Hg resulting in a colorless liquid. Isolated yield: 66.8%. Spectral properties observed: ^1H NMR ($CDCl_3$): δ 1.41 (m, 9H), 1.75 (s, 1H), 2.10 (q, 4H), 3.55 (d, 2H), 4.99 (m, 4H), 5.83 (m, 2H). ^{13}C NMR ($CDCl_3$): δ 26.14, 30.33, 34.08, 40.29, 65.50, 114.41, 138.86. Full characterization described earlier (Valenti 1998).

Synthesis of 2-undec-10-enyl-tridec-12-en-1-ol (**3.9**). To a flame-dried, argon purged 500 mL 3-neck flask equipped with a stir bar, the pure ester **3.7** (9.68 g, 24.6 mmol) was dissolved in 200-225 mL Et_2O. The solution was cooled to 0^oC and 1.0 M LAH/Et_2O solution (62 mL) was added very slowly via syringe. The reaction was then warmed to room temperature and stirred for 6 hr. The reaction was transferred to a large beaker and the LAH was quenched very slowly with deionized water (dropwise addition) water

under an argon atmosphere. After formation of an unsaturated gel, quenching was completed with slow addition of 3N HCl. The resultant mixture was then extracted 3 times with Et_2O and dried over anhydrous $MgSO_4$, filtered, and concentrated under reduced pressure. The crude product was dried over CaH_2 and distilled at 0.1 mm Hg and collected at 162-163°C. The resultant material was further purified by Buchi Glaskugelrohr distillation in order to remove the desired product higher-boiling impurities and collected at 172-175°C with a vacuum of 0.1 mm Hg resulting in a colorless liquid. Isolated yield: 58.6%. Spectral properties observed: ^{1}H NMR ($CDCl_3$): δ 1.22 (m, 42H), 2.01 (q, 4H), 3.55 (d, 2H), 4.98 (m, 4H), 5.81 (m, 2H). ^{13}C NMR ($CDCl_3$): δ 26.87, 28.92, 29.12, 29.47, 29.58, 30.04, 33.79, 40.51, 66.67, 114.06, 139.19. EI/HRMS: calc'd for $C_{24}H_{46}O$: 350.63, found: 350.35. Anal calc'd for $C_{24}H_{46}O$: 82.28 C, 13.14 H; found 82.06 C, 13.36 H.

MEM Substitution. Synthesis of 6-(2-methoxyethoxy-methoxymethyl)- undeca-1,10-diene (**3.10**). Primary alcohol **3.8** (2.55 g, 14.0 mmol) was dissolved in THF (125-150 mL) in a flame-dried, argon purged 250 mL 3-neck flask equipped with a stir bar and condenser. The solution was cooled to 0°C and 1.6 M *n*-BuLi (9.6 mL) was added via syringe over 5-10 min. The solution was stirred for approximately for 30 min at 0°C and warmed to room temperature. After an additional 30 min of stirring, the reaction was recooled to 0°C and methoxyethoxymethyl chloride (2.09 g, 16.8 mmol) was added via a syringe. The solution was warmed to room temperature and the reaction was monitored by TLC for 17-19 hr. The reaction was quenched with 3N HCl, washed 3 times with deionized water, extracted 3 times with Et_2O, and dried over $MgSO_4$. The combined organics were filtered and concentrated under reduced pressure. The product was

purified by flash chromatography through silica gel with a 3:1 ratio of ethyl acetate:hexanes, $R_f = 0.81$ resulting in a colorless liquid. Isolated yield: 35.6%. Spectral properties observed: ^{1}H NMR ($CDCl_3$): δ 1.34 (m, 9H), 1.99 (q, 4H), 3.36 (s, 3H), 3.40 (d, 2H), 3.54 (t, 2H), 3.65 (t, 2H), 4.67 (s, 2H), 4.93 (m, 4H), 5.73 (m, 2H). ^{13}C NMR ($CDCl_3$): δ 26.13, 30.83, 34.09, 38.06, 58.98, 66.65, 70.70, 71.76, 95.62, 114.31, 138.90. EI/HRMS $[M+1]^+$ calc'd for $C_{16}H_{31}O_3$: 271.22, found: 271.23. Anal. cal'd for $C_{16}H_{31}O_3$: 71.06 C, 11.20 H; found 71.45 C, 11.05 H

Cationic ROP. Synthesis of propylene oxide macromonomer (**3.28**). Primary alcohol **3.8** (2.19 g, 12.0 mmol), was dissolved in THF (100-120 mL) in a flame-dried, argon purged 250 mL 3-neck flask equipped with a stir bar, and condenser, and addition funnel. A high-pressure of argon was maintained during addition of tetrafluoroboric acid (0.05 g, 0.30 mmol) via syringe. Care was taken to maintain the solution at room temperature during the subsequent dropwise addition of propylene oxide (4.15 g, 71.6 mmol) via an addition funnel. Caution must be taken due to the highly exothermic process. After addition of propylene oxide, the mixture was warmed to room temperature and stirred under argon for 24 hr. The reaction was quenched with calcium oxide, dissolved in CH_2Cl_2, filtered and concentrated. Isolated yield: 67.7%. Spectral properties observed: ^{1}H NMR ($CDCl_3$): δ 1.13 (m, 12H), 1.33 (m, 8H), 1.59 (m, 1H), 1.99 (q, 4H), 3.48 (m, 14H), 4.95 (m, 4H), 5.79 (m, 2H). ^{13}C NMR ($CDCl_3$): δ 17.17, 18.04, 26.05, 30.76, 34.02, 37.91, 38.21, 66.07, 72.20, 73.28, 75.16, 114.15, 138.87.

Anionic ROP. Synthesis of short chain poly(ethylene oxide) macromonomer (**3.42**). To a flame-dried, argon purged 250 mL 3-neck flask equipped with a stir bar and condenser, primary alcohol **3.8** (0.30 g, 1.6 mmol) was added via syringe and dissolved

in THF (100-125 mL). Subsequently, a 0.3 M solution of potassium naphthalenide (5.5 mL) was added via syringe and the solution was stirred for 30 min at room temperature to maintain a light green color. The color indicated that a slight excess of potassium naphthalenide was present. The solution was cooled to –78°C and condensed ethylene oxide (1.85 g, 42.1 mmol) was added to the reaction via a calibrated burret. Upon completion of EO addition, the reaction mixture was brought to room temperature and stirred for 30 min. The mixture was then brought to 45°C and stirred for 24 hr. The solution was then cooled to room temperature and quenched with acidic MeOH. The organic layer was dissolved in $CHCl_3$, washed with 3 times with deionized water and concentrated under reduced pressure. The resulting product was placed under vacuum (0.1 mm Hg) at 65°C for 4 days to remove residual naphthalene resulting in a yellow oil. Isolated yield: 35.5%. Spectral properties observed: ^{1}H NMR ($CDCl_3$): δ 1.37 (m, 9H), 1.58 (s, 1H), 2.10 (q, 4H), 3.34 (d, 2H), 3.56 (m, 32H), 4.98 (m, 4H), 5.82 (m, 2H). ^{13}C NMR ($CDCl_3$): δ 25.76, 30.50, 33.78, 37.57, 60.96, 70.20, 72.20, 74.19, 113.92, 138.62. EI/HRMS $[M+1]^+$ calc'd for $C_{28}H_{55}O_9$: 535.38, found 535.39. Anal. calc'd for $C_{28}H_{55}O_9$: 62.92 C, 10.11 H; found 61.30 C, 10.00 H. GPC: M_n = 190, PDI = 1.42.

Synthesis of extended poly(ethylene oxide) macromonomer (**3.43**). To a flame-dried, argon purged 250 mL 3-neck flask equipped with a stir bar and condenser, primary alcohol **3.8** (0.30 g, 1.6 mmol) was added via syringe and dissolved in THF (100-125 mL). Subsequently, a 0.3 M solution of potassium naphthalenide (5.5 mL) was added via syringe and the solution stirred for 30 min at room temperature to maintain a light green color. The color indicated that a slight excess of potassium naphthalenide was present. The solution was cooled to –78°C and condensed ethylene oxide (2.94 g, 67.0 mmol) was

added to the reaction via a calibrated burret. Upon completion of EO addition, the reaction was brought to room temperature and stirred for 30 min. Subsequently, the reaction vessel was taken to 45°C and stirred for 24 hr. The solution was then cooled to room temperature and quenched with acidic MeOH. The organic layer was dissolved in $CHCl_3$, washed 3 times with deionized water, and concentrated under reduced pressure. The resulting product was placed under vacuum (0.1 mm Hg) at 65°C for 4 days to remove residual napthalene resulting in a yellow oil. Isolated yield: 51.2%. Spectral properties observed: ^{1}H NMR ($CDCl_3$): δ 1.33 (m, 12H), 2.00 (s, 4H), 3.28 (q, 4H), 3.38 (d, 2H), 3.62 (m, 34H), 5.39 (m, 2H). ^{13}C NMR ($CDCl_3$): δ 17.74, 25.94, 26.79, 29.66, 30.69, 32.82, 61.40, 70.35, 72.52, 130.12, 131.85. Anal. calc'd for $C_{52}H_{101}O_{21}$: 58.81 C, 9.51 H; found 55.48 C, 9.57 H. MALDI-TOF: M_n = 1270, PDI = 1.06. DSC: T_g = -85°C, T_{cc} (onset) = -67°C, T_{cc} (peak) = -61°C, T_m (onset) = -7°C, T_m (peak) = 8°C.

ADMET Polymerization of Polyethylene Oxide Based Macromonomers

Synthesis of a (Polyalchohol). ADMET polymerization of 2-(4-pentenyl)-hept-6-en-1-ol. Monomer (**3.8**) was dried over CaH_2, vacuum transferred, and degassed by 3 freeze-pump-thaw cycles prior to use. Monomer **3.8** (0.30 g, 1.6 mmol) was added to a flame-dried, argon purged 50 mL round bottom flask equipped with a stir bar in an argon atmosphered dry box. Grubbs' second generation benzylidene ruthenium catalyst (0.014 g, 0.016 mmol) was combined with monomer **3.8**. The flask was then fitted with a Teflon™ vacuum valve, sealed, removed from the dry box, and immediatley placed on the vacuum line. The sealed reaction vessel was then exposed to intermittent vacuum for 3 hr at room temperature. After this period of time, the reaction was slowly exposed to full vacuum (0.1 mm Hg) to avoid bumping of the monomer and heated at 45°C for 48 hr.

The temperature was increased to 65°C upon a noticieable viscosity increase and the reaction stirred for an additional 72 hr. Upon completion of the polymerization, the majority of residual catalyst was removed by dissolving the polymer in $CHCl_3$ and adding 1.0 M THP solution (0.4 mL). This solution was heated to 55°C and stirred overnight under an argon atmosphere. The reaction was washed with deionized water until the organic layer was colorless, followed by washing with $NaHCO_3$ until the aqueous layer was slightly basic, dried with $NaSO_3$, and finally concentrated under reduced pressure. Isolated yield: 75.7%. Spectral properties observed: ^{1}H NMR ($CDCl_3$): δ 1.35 (m, 8H), 1.98 (4H), 3.50 (m, 2H), 5.39 (m, 2H). ^{13}C NMR ($CDCl_3$): δ 17.91, 26.83, 27.56, 29.92, 30.37, 32.90, 39.87, 40.34, 65.37, 129.92, 130.41. GPC: M_n = 1700, PDI = 1.94. DSC: T_g = -32°C. Full characterization described earlier (Valenti 1998).

ADMET polymerization of 2-undec-10-enyl-tridec-12-en-1-ol. Monomer **3.9** was prepared and polymerized in the same manner as the previous entry. Isolated yield: 61.2%. Spectral properties observed: ^{1}H NMR ($CDCl_3$): δ 1.40 (m, 34H), 1.98 (4H), 3.54 (m, 2H), 5.36 (m, 2H). ^{13}C NMR ($CDCl_3$): δ 26.91, 29.18, 29.68, 30.10, 30.92, 32.61, 40.51, 65.67, 130.36. Anal calc'd for $C_{22}H_{42}O$: 81.99 C, 13.04 H; found 71.15 C, 11.97 H. GPC: M_n = 10 300, PDI = 2.25. DSC: T_g = -32°C, T_m (onset) = 12°C, T_m (peak) = 22°C.

Synthesis of short chain polyether graft copolymers. ADMET polymerization of 6-(2-methoxy-ethoxymethoxymethyl)-undeca-1,10-diene (**3.12**). Monomer **3.10** was prepared and polymerized in the same manner as the previous entry. Spectral properties observed: ^{1}H NMR ($CDCl_3$): δ 1.32 (m, 12H), 1.96 (m, 4H), 3.36 (s, 3H), 3.42 (d, 2H),

3.61 (t, 2H), 3.68 (t, 2H), 5.38 (m, 2H). ^{13}C NMR ($CDCl_3$): δ 14.19, 23.48, 25.57, 26.94, 31.02, 33.03, 38.16, 59.01, 66.66, 70.74, 71.82, 95.65, 129.81, 130.30. CI/HRMS: calc'd for $C_{16}H_{30}O_2$: 271.22; found 271.22. Anal calc'd for $C_{16}H_{30}O_3$: 71.06 C, 11.20 H; found 71.45 C, 11.05 H. GPC: M_n = 14 400, PDI = 2.23. DSC: T_g = -90°C.

ADMET polymerization of propylene oxide macromonomers (**3.37**). Monomer **3.28** was prepared and polymerized in the same manner as the previous entry. Spectral properties observed: ^{1}H NMR ($CDCl_3$): δ 1.10 (m, 36H), 1.24 (m, 25 H), 1.54 (m, 4H), 1.98 (m, 4H), 3.44 (m, 4H), 4.95 (m, 2H), 5.32 (m, 5H), 5.78 (m, 1H). ^{13}C NMR ($CDCl_3$): δ 17.30, 18.47, 26.13, 26.92, 27.60, 30.89, 32.99, 34.13, 38.04, 38.33, 66.20, 72.32, 73.36, 74.54, 75.21, 114.23, 129.81, 130.27, 139.02. GPC: M_n = 1500, PDI = 2.64.

ADMET polymerization of ethylene oxide macromonomers (**3.44**). The monomer **3.42** was prepared and polymerized in the same manner as the previous entry. Spectral properties observed: ^{1}H NMR ($CDCl_3$): δ 1.42 (m, 9H), 1.62 (s, 1H), 2.08 (q, 4H), 3.38 (d, 2H), 3.60 (m, 80H), 4.94 (m, 4H), 5.79 (m, 2H). ^{13}C NMR ($CDCl_3$): δ 25.99, 30.71, 34.00, 37.78, 61.78, 70.41, 72.53, 74.43, 114.16, 138.86. GPC: M_n = 5500, PDI = 1.45. DSC: T_g = -68°C, T_m (onset) = -54°C, T_m (peak) = -52°C, T_{cc} (peak) = -44°C, T_m (onset) = -15°C, T_m (peak) = 0°C.

Synthesis of Polystyrene Macromonomers

Ester-Alcohol Coupling. Synthesis of 2-bromo-2-methyl-propionic acid 2-pent-4-enyl-hept-6-enyl ester (**4.28**). To a 50 mL 3-neck round bottom flask were added 1-bromo-2,2'-dimethyl propionic acid (1.95 g, 11.7 mmol), and EDC·HCl (2.24 g, 11.7 mmol). These materials were then dissolved in 25 mL of CH_2Cl_2 and cooled to 0°C.

Primary alcohol **3.8** (1.0 g, 5.5 mmol) was then added via syringe and the solution stirred for 2 hr at 0°C under an argon flow. DMAP (0.06 g, 0.49 mmol) was added, the solution warmed to room temperature, and subsequently stirred overnight, at which point the reaction mixture became a faded brown/yellow in color. The reaction was quenched with saturated $NaHCO_3$, washed 3 times with deionized water, and extracted 3 times with Et_2O. The organic layer was then dried with anhydrous $MgSO_4$, filtered and concentrated. The crude product was purified by flash chromatography using silica gel with a 1:1 ratio of hexanes:ethyl acetate, $R_f = 0.74$ resulting in a colorless liquid. Isolated yield: 98.0%. Spectral properties observed: ^1H NMR ($CDCl_3$): δ 1.36 (m, 8H), 1.90 (s, 6H), 2.02 (q, 4H), 4.08 (d, 2H), 4.94 (m, 4H), 5.76 (m, 2H). ^{13}C NMR ($CDCl_3$): δ 26.01, 30.74, 30.84, 33.91, 37.24, 68.51, 114.54, 138.61. EI/HRMS: FAB calc'd for $C_{16}H_{27}O_2Br$: 331.13, found: 331.13. Anal calc'd for $C_{16}H_{27}O_2Br$: 58.01 C, 8.16 H, 24.17 Br; found 58.28 C, 8.20 H, 23.54 Br.

Synthesis of 2-bromo-2-methyl-propionic acid 2-undec-enyl-tridec-12-enyl ester (**4.29**). To a 50 mL 3-neck round bottom flask were added 1-bromo-2,2'-dimethyl propionic acid (1.01 g, 6.1 mmol), and EDC·HCl (1.16 g, 6.1 mmol). These materials were then dissolved in 25 mL of CH_2Cl_2 and cooled to 0°C. Primary alcohol **3.9** (1.0 g, 2.9 mmol) was then added via syringe and the solution stirred for 2 hr at 0°C under an argon flow. DMAP (0.03 g, 0.26 mmol) was added, the solution warmed to room temperature, and subsequently stirred overnight, at which point the reaction mixture became a faded brown/yellow in color. The reaction was quenched with saturated $NaHCO_3$, washed 3 times with deionized water, and extracted 3 times with Et_2O. The organic layer was then dried with anhydrous $MgSO_4$, filtered and concentrated. The

crude product was purified by flash chromatography using silica gel with 9:1 ratio of hexanes:ethyl acetate, R_f = 0.64 resulting in a colorless liquid. Isolated yield: 84.6%. Spectral properties observed: ^{1}H NMR ($CDCl_3$): δ 1.35 (m, 32H), 1.91 (s, 6H), 2.05 (q, 4H), 4.08 (d, 2H), 4.98 (m, 4H), 5.81 (m, 2H). ^{13}C NMR ($CDCl_3$): δ 14.081, 22.63, 26.63, 28.92, 29.11, 29.52, 29.88, 30.77, 31.19, 33.78, 37.27, 55.91, 68.58, 114.07, 139.15, 171.72. CI/HRMS: calc'd for $C_{28}H_{52}O_2Br$: 499.31, found 499.31. Anal calc'd for $C_{28}H_{52}O_2Br$: 67.25 C, 10.21 H; found 67.37 C, 10.30 H.

ATRP of Styrene. Synthesis of short chain polystyrene macromonomer (**4.33**). Copper (I) bromide (0.43 g, 3.0 mmol) and bipy (0.94 g, 6.0 mmol) were weighed out and placed into a flame-dried, argon purged 50 mL Schlenk tube equipped with a stir bar. Diphenyl ether (5 mL) was added via syringe and the mixture was subsequently degassed with 3 freeze-pump-thaw cycles. Initiator **4.29** (0.75 g, 1.5 mmol) and styrene (3.63 g, 22.5 mmol) were next added via syringe to aforementioned solution. The resultant mixture was stirred for 3 hr at 110°C while maintaining a slight argon flow. The solution changed from brown to green upon heating. The reaction mixture was cooled to room temperature and quenched with THF (60 mL), filtered through a neutral bed of alumina in order to remove residual catalyst, and filtrate was concentrated to 30 mL. Macromonomer **4.33** was obtained by precipitation into cold MeOH. Finally, this solution was filtered and the white solid product, **4.33**, was dried under reduced pressure at 50°C for 24 hr. Isolated yield: 65.2%. Spectral properties observed: ^{1}H NMR ($CDCl_3$) δ 0.90 (m, 8H), 1.21 (m, 32H), 1.39 (m, 36H), 1.82 (m, 14H), 2.08 (q, 4H), 3.51 (d, 2H), 4.99 (m, 4H), 5.81 (m, 2H), 6.61 (m, 35H), 7.09 (m, 73H). ^{13}C NMR ($CDCl_3$): δ 26.67, 28.93, 29.14, 29.59, 29.96, 31.26, 33.80, 37.02, 40.33, 41.82, 66.81, 114.12, 118.82,

123.13, 125.60, 127.91, 129.66, 139.14, 145.24, 157.16, 177.81. Anal calc'd for $C_{148}H_{171}O_2Br$: 87.27 C, 8.20 H; found 86.71 C, 8.17 H. GPC: M_n = 2 500, PDI = 1.16. MALDI-TOF: M_n = 2200, PDI = 1.16. DSC: T_g = 20°C.

Synthesis of Extended Chain Polystyrene Macromonomer (**4.34**). Copper (I) bromide (0.11 g, 0.80 mmol) and bipy (0.25 g, 1.6 mmol) were weighed out and placed into a flame-dried, argon purged 50 mL Schlenk tube equipped with a stir bar. Diphenyl ether (5 mL) was added via syringe and the mixture was subsequently degassed with 3 freeze-pump-thaw cycles. Initiator **4.29** (0.20 g, 0.40 mmol) and styrene (1.93 g, 12.0 mmol) were next added via syringe to aforementioned solution. The resultant mixture was stirred for 3 hr at 110°C while maintaining a slight argon flow. The solution changed from brown to green upon heating. The reaction mixture was cooled to room temperature and quenched with THF (40 mL), filtered through a neutral bed of alumina in order to remove residual catalyst, and filtrate was concentrated to 25 mL. Macromonomer **4.34** was obtained by precipitation into cold MeOH. Finally, this solution was filtered and the white solid product, **4.34**, was dried under reduced pressure at 50°C for 24 hr. Isolated yield: 58.4% Spectral properties observed: ^{1}H NMR ($CDCl_3$): δ 0.99 (m, 16H), 1.25 (m, 36H), 1.40 (m, 48H), 1.88 (m, 20H), 2.10 (q, 4H), 3.57 (d, 2H), 4.97 (m, 4H), 5.84 (m, 2H), 6.65 (m, 60H), 7.12 (m, 90H). ^{13}C NMR ($CDCl_3$): δ 26.59, 28.89, 29.08, 29.54, 29.99, 31.30, 33.76, 36.98, 40.41, 41.88, 66.80, 114.08, 118.90, 123.10, 125.55, 127.90, 129.62, 139.09, 145.20, 157.01, 177.40. Anal calc'd for $C_{268}H_{291}O_2Br$: 88.29 C, 8.10 H; found 88.08 C, 8.09 H. GPC: M_n = 3000, PDI = 1.14. MALDI-TOF: M_n = 2800, PDI = 1.26. DSC: T_g = 35°C.

ADMET Polymerization of Polystyrene Macromonomers and Initiators

ADMET polymerization of 2-bromo-2-methyl-propionic acid 2-pent-4-enyl-hept-6-enyl ester **(4.30)**. Monomer **4.28** was prepared and polymerized in the same manner as previously ADMET described polymerizations. Spectral properties observed: ^{1}H NMR ($CDCl_3$): δ 1.39 (m, 8H), 1.71 (m, 1H), 1.90 (s, 6H), 1.98 (m, 4H), 4.05 (d, 2H), 5.39 (m, 2H). ^{13}C NMR ($CDCl_3$): δ 26.63, 30.76, 32.76, 37.11, 68.38, 130.22, 171.67. Anal calc'd for $C_{14}H_{20}O_2Br$: 56.00 C, 6.67 H; found 53.50 C, 7.37 H. GPC: M_n = 46 500, PDI = 2.17. DSC: T_g = -50°C.

ADMET polymerization of 2-bromo-2-methyl-propionic acid 2-undec-enyl-tridec-12-enyl ester **(4.31)**. Monomer **4.29** was prepared and polymerized in the same manner as previously described ADMET polymerizations. Synthesized as above. Spectral properties observed: ^{1}H NMR ($CDCl_3$): δ 1.41 (m, 36H), 1.79 (m, 1H), 2.00 (s, 6H), 2.05 (m, 4H), 4.10 (d, 2H), 5.37 (m, 2H). ^{13}C NMR ($CDCl_3$): δ26.66, 29.19, 29.52, 29.59, 29.66, 29.91, 30.79, 31.21, 37.28, 55.96, 68.60, 130.31, 171.75. Anal calc'd for $C_{26}H_{47}O_2Br$: 66.24 C, 9.98 H; found 64.42 C, 10.00 H. GPC: M_n = 33 800, PDI = 2.05. DSC: T_g = -67°C, T_m (onset) = -13°C, T_m (peak) = -9°C.

ADMET polymerization of short chain polystyrene macromonomer **(4.35)**. Macromonomer **4.33** (0.23 g, 0.092 mmol) was added to a flame-dried, argon purged 50 mL Schlenk tube equipped with a stir bar in the dry box. Grubbs' second generation benzylidene ruthenium catalyst (0.001 g, 0.001 mmol) was next added to **4.33** and the Schlenk tube sealed. The reaction flask was removed from the dry box and immediately placed under a slight argon flow. Toluene (1 mL) was added via syringe to dissolve the macromonmer and the reaction mixture was heated with stirring to 75°C. The reaction

was monitored by ^{1}H NMR and slowly stirred for 10 days, until completion of the reaction (Note: new catalyst was added after 5 days and fresh toluene was added approximately every 24 hr to maintain solution conditions). Upon cooling to room temperature, this mixture was precipitated into cold MeOH. The resultant polymer, **4.35**, was collected and dried under vacuum at 50°C for 48 hr. Spectral properties observed: ^{1}H NMR ($CDCl_3$): δ 0.98 (m, 5H), 1.43 (m, 36H), 1.98 (m, 12H), 2.38 (s, 8H), 5.39 (m, 2H), 6.67 (m, 17H), 7.18 (m, 50H). ^{13}C NMR ($CDCl_3$): δ 29.59, 32.59, 40.33, 41.77, 50.51, 125.59, 127.91, 130.28, 145.25. Anal calc'd for $C_{146}H_{167}O_2Br$: 86.27 C, 8.22 H; found 85.48 C, 8.08 H. GPC: M_n = 10 400, PDI = 4.85. DSC: T_g = 60°C.

ADMET polymerization of extended chain polystyrene macromonomer (**4.36**). Macromonomer **4.34** was prepared and polymerized in the same manner as the previous entry. Spectral properties observed: ^{1}H NMR ($CDCl_3$): δ 0.98 (m, 6H), 1.41 (m, 38H), 1.96 (m, 14H), 2.39 (s, 2H), 3.45 (m, 1H), 4.43 (m, 2H), 5.39 (m, 2H), 6.69 (m, 26H), 7.20 (m, 48H). ^{13}C NMR ($CDCl_3$): δ 27.48, 29.65, 40.42, 41.50, 44.04, 46.32, 125.65, 127.95, 129.04, 145.24. Anal calc'd for $C_{266}H_{287}O_2Br$: 88.89 C, 7.99 H; found 86.77 C, 8.11 H. GPC: M_n = 6300, PDI = 4.80. DSC: T_g = 60°C.

Copolymerization of Polystyrene Macromonomers with 1,9-Decadiene

Synthesis of 75 mol% of short chain polystyrene macromonomer and 25 mol% 1,9-decadiene (**5.4**). Macromonomer **4.33** (0.12 g, 0.05 mmol) and 1,9-decadiene (0.002 g, 0.012 mmol) were combined in a flame-dried, argon purged 50 mL Schlenk tube equipped with a stir bar and Teflon™ valve vacuum adapter an argon atmosphere dry box. Grubbs' second generation benzylidene catalyst (0.001 g, 0.001 mmol) was then added to and removed from the dry box. The reaction was placed under an argon flow

and toluene (1 mL) was added to the reaction. The reaction was heated to 75°C and stirred for 10 days. Fresh toluene was added every 24 hr to maintain solution conditions and fresh catalyst (0.001 g, 0.001 mmol) was added after 5 days. Upon completion of the reaction as indicated by ^{1}H NMR, the polymer was precipitated into cold MeOH, filtered, and dried under vacuum (0.1 mm Hg) at 50°C for 48 hr. Spectral properties observed: ^{1}H NMR ($CDCl_3$): δ 0.95 (m, 4H), 1.21 (m, 50H), 1.98 (m, 16H), 3.58 (d, 2H), 5.38 (m, 4H), 6.61 (m, 18H), 7.18 (m, 40H). ^{13}C NMR ($CDCl_3$): δ 26.15, 27.01, 29.32, 30.12, 31.92, 32.55, 39.87, 40.12, 41.02, 124.78, 125.68, 128.02, 129.89, 131.33, 144.12, 145.19. Anal calc'd for $C_{446}H_{461}O_6Br_3$: 87.04 C, 7.68 H; found 87.07 C, 8.66 H. GPC: M_n = 13 800, PDI = 3.59. DSC: T_g= 14°C.

Synthesis of 50 mol% of short chain polystyrene macromonomer and 50 mol% 1,9-decadiene (**5.5**). Macromonomer **4.33** (0.14 g, 0.06 mmol) and 1,9-decadiene (0.008 g, 0.06 mmol) were combined in a flame-dried, argon purged 50 mL Schlenk tube equipped with a stir bar and Teflon™ valve vacuum adapter an argon atmosphere dry box. Grubbs' second generation benzylidene catalyst (0.001 g, 0.001 mmol) was then added to and removed from the dry box. The reaction was placed under an argon flow and toluene (1 mL) was added to the reaction. The reaction was heated to 75°C and stirred for 10 days. Fresh toluene was added every 24 hr to maintain solution conditions and fresh catalyst (0.001 g, 0.001 mmol) was added after 5 days. Upon completion of the reaction as indicated by ^{1}H NMR, the polymer was precipitated into cold MeOH, filtered, and dried under vacuum (0.1 mm Hg) at 50°C for 48 hr. Spectral properties observed: ^{1}H NMR ($CDCl_3$): δ 0.99 (m, 28H), 1.38 (m, 120H), 2.06 (m, 42H), 3.52 (d, 2H), 5.01 (m, 2H), 5.41 (m, 10H), 5.81 (m, 1H), 6.63 (m, 40H), 7.19 (m, 90H). ^{13}C NMR ($CDCl_3$): δ

26.68, 26.91, 29.22, 29.68, 30.01, 31.09, 32.56, 40.21, 40.87, 41.76, 125.66, 127.58, 128.94, 129.19, 130.00, 144.65, 145.32. Anal calc'd for $C_{178}H_{205}O_2Br$: 87.04 C, 8.36 H; found 86.44 C, 8.78 H. GPC: M_n = 7500, PDI = 1.95. DSC: $T_g = 20^oC$.

Synthesis of 25 mol% of short chain polystyrene macromonomer and 75 mol% 1,9-decadiene (**5.6**). Macromonomer **4.33** (0.12 g, 0.05 mmol) and 1,9-decadiene (0.03 g, 0.20 mmol) were combined in a flame-dried, argon purged 50 mL Schlenk tube equipped with a stir bar and Teflon™ valve vacuum adapter an argon atmosphere dry box. Grubbs' second generation benzylidene catalyst (0.002 g, 0.002 mmol) was then added to and removed from the dry box. The reaction was placed under an argon flow and toluene (1 mL) was added to the reaction. The reaction was heated to 75°C and stirred for 10 days. Fresh toluene was added every 24 hr to maintain solution conditions and fresh catalyst (0.002 g, 0.002 mmol) was added after 5 days. Upon completion of the reaction as indicated by ^1H NMR, the polymer was precipitated into cold MeOH, filtered, and dried under vacuum (0.1 mm Hg) at 50°C for 48 hr. Spectral properties observed: ^1H NMR ($CDCl_3$): δ 0.92 (m, 22H), 1.20 (m, 170H), 1.99 (m, 55H), 3.55 (d, 2H), 5.39 (m, 16H), 6.58 (m, 53H), 7.09 (m, 116H). ^{13}C NMR ($CDCl_3$): δ 24.76, 25.89, 27.08, 28.01, 29.00, 30.67, 31.12, 31.96, 40.89, 41.70, 124.80, 127.40, 128.99, 129.21, 130.73, 131.44, 145.89, 146.00. Anal calc'd for $C_{218}H_{275}O_2Br$: 87.11 C, 9.16 H; found 85.23 C, 9.00 H. GPC: M_n = 11 600, PDI = 2.87. DSC: Tg = 23°C.

Synthesis of 75 mol% of extended chain polystyrene macromonomer and 25 mol% 1,9-decadiene (**5.8**). Macromonomer **4.34** (0.10 g, 0.03 mmol) and 1,9-decadiene (0.001 g, 0.008 mmol) were combined in a flame-dried, argon purged 50 mL Schlenk tube equipped with a stir bar and Teflon™ valve vacuum adapter an argon atmosphere dry

box. Grubbs' second generation benzylidene catalyst (0.001 g, 0.001 mmol) was then added to and removed from the dry box. The reaction was placed under an argon flow and toluene (1 mL) was added to the reaction. The reaction was heated to 75°C and stirred for 10 days. Fresh toluene was added every 24 hr to maintain solution conditions and fresh catalyst (0.001 g, 0.001 mmol) was added after 5 days. Upon completion of the reaction as indicated by ^{1}H NMR, the polymer was precipitated into cold MeOH, filtered, and dried under vacuum (0.1 mm Hg) at 50°C for 48 hr. Spectral properties observed: ^{1}H NMR ($CDCl_3$): δ 0.95 (m, 22H), 1.20 (m, 144H), 1.90 (m, 45), 3.45 (d, 2H), 5.36 (m, 14H), 6.60 (m, 42H), 7.10 (m, 92H). ^{13}C NMR ($CDCl_3$): δ 26.70, 27.21, 29.04, 29.38, 30.03, 31.32, 32.61, 40.37, 41.80, 99.46, 125.64, 127.68, 128.42, 129.89, 130.34, 145.00, 145.42. Anal calc'd for $C_{814}H_{889}O_6Br_3$: 87.04 C, 7.68 H; found 87.07 C, 8.66 H. GPC: M_n = 13 600, PDI = 4.34. DSC: T_g = 44°C.

Synthesis of 50 mol% of extended chain polystyrene macromonomer and 50 mol% 1,9-decadiene (**5.9**). Macromonomer **4.34** (0.14 g, 0.05 mmol) and 1,9-decadiene (0.006 g, 0.04 mmol) were combined in a flame-dried, argon purged 50 mL Schlenk tube equipped with a stir bar and Teflon™ valve vacuum adapter an argon atmosphere dry box. Grubbs' second generation benzylidene catalyst (0.001 g, 0.001 mmol) was then added to and removed from the dry box. The reaction was placed under an argon flow and toluene (1 mL) was added to the reaction. The reaction was heated to 75°C and stirred for 10 days. Fresh toluene was added every 24 hr to maintain solution conditions and fresh catalyst (0.001 g, 0.001 mmol) was added after 5 days. Upon completion of the reaction as indicated by ^{1}H NMR, the polymer was precipitated into cold MeOH, filtered, and dried under vacuum (0.1 mm Hg) at 50°C for 48 hr. Spectral properties observed: ^{1}H

NMR ($CDCl_3$): δ 0.99 (m, 32H), 1.25 (m, 232H), 1.98 (m, 72H), 3.51 (d, 2H), 5.40 (m, 24H), 6.58 (m, 89H), 7.10 (m, 154H). ^{13}C NMR ($CDCl_3$): δ 25.67, 26.27, 27.98, 29.35, 29.98, 30.13, 31.14, 32.56, 39.97, 41.10, 126.04, 127.15, 128.00, 128.56, 129.72, 130.08, 144.89, 145.22. Anal calc'd for $C_{209}H_{329}O_2Br$: 88.75 C, 8.39 H; found 87.18 C, 8.91 H. GPC: M_n = 8000, PDI = 3.95. T_m (onset) = 23°C, T_m (peak) = 39°C.

Synthesis of 25 mol% of extended chain polystyrene macromonomer and 75 mol% 1,9-decadiene **(5.10)**. Macromonomer **4.34** (0.02 g, 0.06 mmol) and 1,9-decadiene (0.01 g, 0.08 mmol) were combined in a flame-dried, argon purged 50 mL Schlenk tube equipped with a stir bar and Teflon™ valve vacuum adapter an argon atmosphere dry box. Grubbs' second generation benzylidene catalyst (0.001 g, 0.001 mmol) was then added to and removed from the dry box. The reaction was placed under an argon flow and toluene (1 mL) was added to the reaction. The reaction was heated to 75°C and stirred for 10 days. Fresh toluene was added every 24 hr to maintain solution conditions and fresh catalyst (0.001 g, 0.001 mmol) was added after 5 days. Upon completion of the reaction as indicated by ^1H NMR, the polymer was precipitated into cold MeOH, filtered, and dried under vacuum (0.1 mm Hg) at 50°C for 48 hr. Spectral properties observed: ^1H NMR ($CDCl_3$): δ 1.00 (m, 16H), 1.19 (m, 298H), 2.01 (m, 110H), 3.53 (d, 2H), 5.41 (m, 25H), 6.61 (m, 97H), 7.09 (m, 199H). ^{13}C NMR ($CDCl_3$): δ 24.99, 25.75, 26.72, 29.08, 29.75, 30.80, 31.22, 32.60, 40.19, 41.19, 126.04, 127.15, 128.00, 128.56, 129.53, 129.91, 130.08, 145.00, 145.82. Anal calc'd for $C_{338}H_{413}O_2Br$: 88.54 C, 9.02 H; found 85.76 C, 9.22 H. GPC: M_n = 9400, PDI = 4.37. DSC: T_m (onset) = 33°C, T_m (peak) = 39°C.

CHAPTER 3
POLYETHER GRAFT COPOLYMERS

Structure control in polymer synthesis is obviously important to all interested in creating new materials. Given the constraints associated with synthesizing polymers possesing entirely new repeat units, modern focus is often on intriguing polymeric architectures made from common monomers such as those produced from typical chain and step polymerizations (Kobatake et al. 1998, Edgecombe et al. 1998). The material presented demonstrates an innovative graft architecture for the assembly of polyolefin and polyether repeat units; the preparation of "perfect" combs wherein the *teeth* are essentially comprised of monodisperse poly(ethylene oxide) and the *backbone* is an unsaturated polyolefin. Furthermore, the run length between adjacent teeth is exact along the polyolefin backbone in part to the precise manner of the sythesis.

Macromonomer Design

It is evident that controlling each aspect of a polymerization scheme can alter the resulting polymer's topology, composition, or placement of functional groups at various sites along the polymer. One topology of particular interest is the graft copolymer array. Creating this architecture is challenging since the synthesis of copolymers with precise placement of the graft has been documented as being a nontrivial target when using typical polymerization methods (Burchard 1999).

Polyether grafts are of specific interest because of their structural similarity to poly(ethylene oxide) (PEG). PEG is a nontoxic, biocampatible, and highly water-soluble

material. The combination of hydrophilic polyethers grafted onto a polyolefin backbone proves to be an interesting application for exploration. These polyethene-based materials will have an increased solubility in polar solvents due to the polyether grafts. Furthermore, grafted PEG materials are known to be valuable in biomedical applications (Harris 1992, Roberts and Harris 1998, Zhao et al. 1998) and are also known as compatibilizers in polymer blending (Hallden et al. 2000). However, the first reports to enhance polymer performance by precise spacing were outlined in the synthesis of "perfect comb" polyethylene-g-polyether copolymers (O'Donnell et al. 2001).

It is acknowledged that acyclic diene metathesis (ADMET) successfully yields high molecular weight, linear, unsaturated polymers possessing various functional groups, both within and pendant to the polymer backbone (Figure 3-1). If desired, these functional groups can be placed at exact intervals along the polymer backbone, something that has been previously demonstrated (Valenti and Wagener 1998, Watson and Wagener 2000a, 2000b). Consequently, the goal of this research has been to exploit ADMET in the preparation of novel graft copolymer structures.

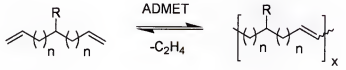

R = OH, Me, (C)=O, Cl, Ph, OAc, CO_2Me, CO_2Et

Figure 3-1. ADMET polymerization of functionalized macromonomers.

Monomer design is central to this work. The method to creating perfect comb polymers involves inserting the graft a priori into a symmetrical α,ω-diene before ADMET polymerization. This requires we invoke the macromonomer approach in step

polymerization chemistry. Macromonomers are typically found in chain polymerization, and in fact have been used to produce graft copolymers in various chain polymerization schemes (Mercerryes et al. 1999, Shinoda et al. 2001). In this case the grafts are usually packed tightly together (in vinyl monomer homopolymerization), or they are randomly distributed in vinyl copolymerization schemes. In the research presented herein, diene macromonomers are converted to polymers via step propagation, condensation-type polymerization (ADMET chemistry) with the distance between graft points precisely being regulated by placing discrete methylene run lengths between them in the monomer.

Substitution Chemistry

The primary approach to produce graft copolymers containing polyether chains was via S_N2 substitution chemistry. The synthesis of graft copolymers possessing both controlled graft length and exact run lengths along the polymer backbone is first achieved by symmetrically positioning the graft within the diene macromonomer itself. These monomer dienes are then converted into true graft copolymers via ADMET chemistry. The synthesis of the grafted symmetrical dienes were initiated with the dialkylation of ethyl acetoacetate (**3**). The keto-ester (**4**or **5**) was decarboxylated through a retro-claisen reaction with sodium ethoxide to form an ester (**6** or **7**) followed by a reduction to the primary alcohol (**8** or **9**) with lithium aluminum hydride (LAH). Short chain polyether grafts are placed along the α,ω-diene via substitution chemistry using methoxyethoxymethyl chloride (MEMCl). This chemistry is clean and leads to a single graft site (**10**) symmetrically placed within each monomer unit (Figure 3-2). Thus, polymerization of the monomer will lead to a graft in each repeat unit via step macromonomer polymerization.

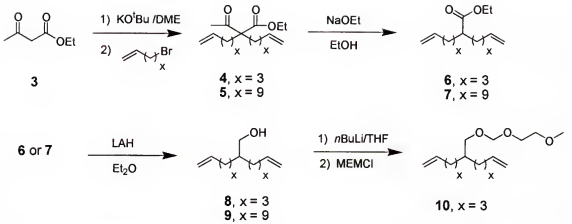

Figure 3-2. Short chain polyether synthetic route.

The short chain polyether macromonomer (**10**) was prepared for polymerization by extensive drying followed by degassing techniques. The diene was then metathesized with Grubbs' first generation benzylidene ruthenium catalyst at room temperature by standard ADMET techniques. Conversion of the macromonomers to the unsaturated polymer (Figure 3-3) was trivial and can be observed by ^{1}H NMR.

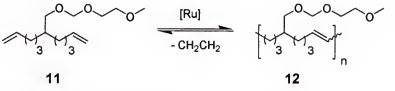

Figure 3-3. ADMET polymerization of short chain polyether grafts.

As the polymerization proceeds, the α,ω-diene terminal olefin peaks at 4.93 and 5.73 ppm decrease in intensity while the internal olefin peak of the unsaturated polyolefin at 5.38 ppm becomes more pronounced. ADMET polymerization was highly successful for short chain polyether graft monomers. End group analysis indicated that the terminal

olefins were no longer observable by NMR techniques; i.e., high molecular weight graft copolymers were formed (Figure 3-4).

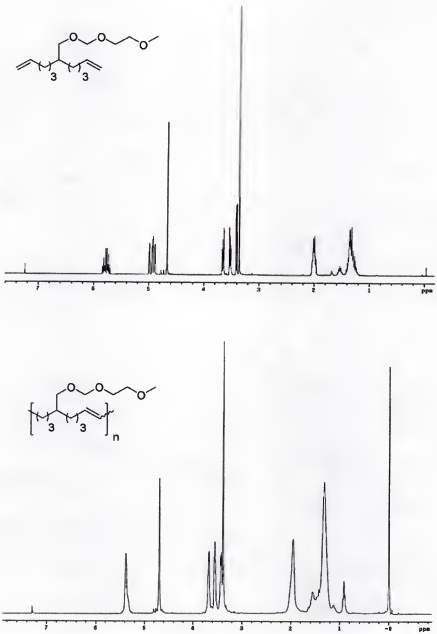

Figure 3-4. ^{1}H NMR spectrum of ADMET polymerization of macromonomer (**10**).

Attempts at attaching longer polyether chains to the diene functionality through substitution methods were also made with PEG chains of M_n = 2,000 and M_n = 5,000.

These approaches involved the conversion of a terminal alcohol on the PEG chain (**13**) to a better leaving group such as a chloride (**14**) or tosylate (**15**). The intent was then to activate the diene by deprotonation of the alcohol (**8**) for substitution of the PEG chain (Figure 3-5). However, these attempts were unsucessful since the PEG alcohol functionalities were unable to be converted to the leaving groups; therfore they could not be further used as an electrophile. Another attempt by substitution involved the conversion of the primary alcohol (**8**) to a tosylate group (**17**). The diene was added in a dropwise manner to a deprotonated PEG chain (**13**) with *n*-BuLi through titration methods. As with previous attempts made by substitution methods, NMR analysis indicated that the reaction was unsuccessful.

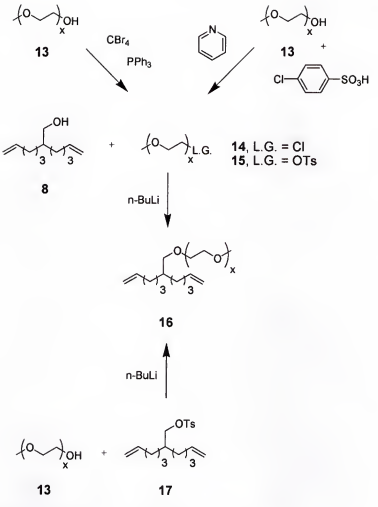

Figure 3-5. Substitution attempts with long chain PEG.

It is often difficult to accomplish chemistry on long chain polymers, and even more so when attempts are made on a single site along an extended polymer chain. Therefore, other options for attaching extended polyether chains to the diene functionality were explored. These investigations involved ionic polymerizations because of their excellent control over polydispersity and extent of polymerization.

Cationic Polymerizations

In order to acquire well-defined systems, "living" polymerizations were explored because of their controlled active chain ends. Cationic polymerizations are initiated by the reaction of an electrophilic cation with an electron-donating molecule. The resulting

monomer cation adds to further monomers if the nucleophilic groups of the monomers reside in a part of the molecule that can participate in the polymerization (Elias 1997). Thus, compounds containing electron rich substituents, heteroatoms, or cyclic molecules containing heteroatoms can be considered for cationic polymerizations. For example, with electron-rich olefin derivatives including π-donors, the initiator cation attacks the most nucleophilic group of the monomer molecule, allowing propagation of the polymer. Some classic ring compounds that are cationically polymerizable are cyclic ethers, imines, acetals, sulfides, esters and amides (Figure 3-6).

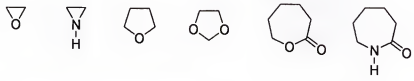

Figure 3-6. Cationic ring opening compounds.

Catioinic Initiation

Most cationic initiations take place by a two-electron heterolytic mechanism. These initiators can be divided into three classifications: carbenuim salts, Bronsted acids, and Lewis acids.

Carbenuim salts dissociate into carbenium ions and counter ions when in solvents used for cationic polymerizations. This dissociation is encouraged by complexation of the counter anion. For example, the dissociation of triphenylcarbenium ion to $(C_6H_5)_3C^+$ and Cl^- is assisted by complexation of the counter anion to form a complex anion such as antimony pentachloride, $SbCl_5$. The chloride anion Cl^- complexes to form a hexachloroantimonate ion $[SbCl_6]^-$. However, the complex anions can be easily

fragmented in which the dissociation products will lead to several side reactions. Non-complex anions such as $[ClO_4]^-$ or $[CF_3SO_3]^-$ do not dissociate, yet they may terminate chains by bonding and creating macrocations.

Bronsted acids dissociate into protons and counter anions in the same manner as with perchloric acid dissociating to H^+ and $[ClO_4]^-$ ions. However, perchloric acid is a covalent compound in oxygen-free solvents and it does dissociate in the presence of Bronsted bases. This acid-base reaction explains that not all proton acids are able to start cationic polymerizations. It is essential that monomer cations do not combine irreversibly with the counter ion; otherwise; low yields of lower molar mass polymer will result. In order to obtain a high molecular weight in high yields, the monomer should be added to the Bronsted acid so that the anions are stabilized by excess acid.

Some Lewis acids are able to undergo self-ionization to form electrical conducting solutions. However, there are other Lewis acids that require "co-catalysts" such as water, trichloroacetic acid, ethers, or the monomer itself to undergo ionization. Cations resulting from these reactions add to monomers and start the polymerization. "Co-catalysts" do not act catalytically but rather provide the initiating species required to form the salt from the Lewis acid (Figure 3-7).

Figure 3-7. Co-catalyst of Lewis acids.

Cationic Propagation

Propagation of cationic polymerizations take place through repeat addition of monomers to an *enium* or *onium ion* (Figure 3-8). *Enium ions* are cations with electron-deficient centers composed of *carbenium ions* (**21**), *dioxolenium ions* (**22**), and *silicenium ions* (**23**). During polymerizations, the highly charged positive center of the *carbenium ion* attacks the partial electronegative charge. Thus, the dipole moment of the transition state is created by the attacking cation which allows for a linear transition state and a low energy of activation. *Oxonium ions* (**24**) are strongly solvated, and their charge density is smaller than *carbenium ions*. The monomers must therefore posses a strong dipole, and since the transition state is not linear, high energies of activation are required. *Carbonium ions* (**25**) are four- or five-fold coordinated, non-classical carbocations that are obtained from enium ions through further addition of ligands. In addition, *carboxonium ions* are formulated by the addition of oxygen to *carbenium ions* and are much more stable than carbocations because of their strong nucleophilic character.

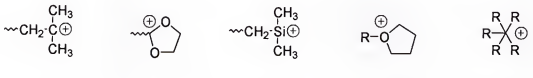

21 **22** **23** **24** **25**

Figure 3-8. Enium and onium ions.

"Living" cationic conditions can be achieved when the carbenium ions are nucleophilically stabilized. One method to reduce the cationic charge is the addition of a counter ion. However, strong Lewis acids do not lead to non-living polymerizations. Even though Lewis acids strongly dissociate into nucleophilic counter ions, they are too

weak to stabilize the growing chain. The acidity of β-protons can be decreased through the addition of a weak Lewis base. However, the effectiveness does depend on pk_a values. As pk_a increases, a "living" polymerization with termination eventually changes to polymers with broader distributions and finally toward no polymerization.

Cationic Termination

Cationic polymerizations exhibit termination by dissociation of the complex or by chain transfer reactions. Since the reactivity of the cations was fairly high, termination by dissociation of the complex counter ion is common (Figure 3-9). Termination can also occur by monomer pairing in which a hydride transfer from the monomer to the cation generates a resonance stabilization that can no longer undergo further polymerization. In addition, chain transfer reactions commonly occur in cationic polymerizations where the transfer of the cation to another monomer initiates further polymerizations. Yet, it terminates polymerization of the original macrocation. This pathway tends to lower molecular weight and broaden polydispersities.

Termination by complex dissociation

Termination by monomer pairing

Chain transfer

Figure 3-9. Cationic terminations and chain transfer.

Propylene Oxide Cationic Ring Opening Polymerization

Upon the examination of cationic ring opening polymerization of propylene oxide, a series of oligomers was prepared (**28**) after slowly adding the diene (**8**) to the activated monomer (**27**) using $HBF_4{\cdot}OEt_2$ as the initiator (Figure 3-10).

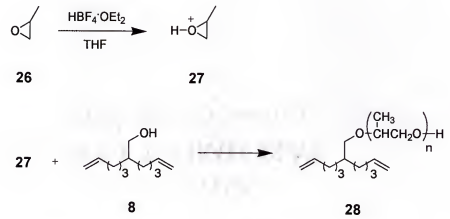

Figure 3-10. Cationic polymerization conditions of propylene oxide.

It is known that significant side reactions take place in the cationic polymerization of cyclic ethers and acetals (Biedron et al. 1995). The reaction of oxygen atoms from the repeat unit react with the growing species located on the growing chain end. A simplistic mechanism accounts for an activated monomer (AM) and involves the attack of the protonated monomer molecule on the hydroxy end-group of the growing macromolecule (**29**) where "H^+" represents a fast proton exchange between all the bases in the system (Figure 3-11). In contrast, the active chain end (ACE) mechanism accounts for the active species, a tertiary oxonium ion (**30**), to be located at the chain end. It is the dissociation of the proton to the neutral chain end of the AM mechanism that minimizes undesirable side reactions such as cyclization or scrambling. Without the presence of the tertiary oxonium ion, it is impossible for scrambling or cyclized products to occur (Brzezinska et al. 1986, Penczek and Kubisa 1993). Thus, in order to eliminate side reactions, it is therefore critical to minimize contributions from the ACE mechanism.

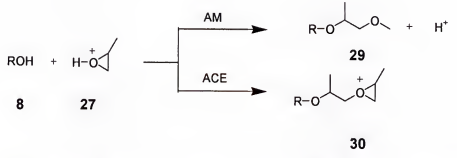

Figure 3-11. Activated Monomer (AM) and Active Chain End (ACE) mechanisms of propylene cationic polymerization.

After cationic ring-opening polymerization of propylene oxide (PO) to the primary alcohol, GPC analysis displayed multiple peaks which indicate the presence of several PPO chains of various lengths were present. These different chains can be explained

through the ACE mechanism in which a "back-biting" effect occurs (Figure 3-12). This phenonmenon is known to proceed in hydroxy based polyether cationic polymerizations that tend to undergo intramolecular cyclizations (Bednarek et al. 2001).

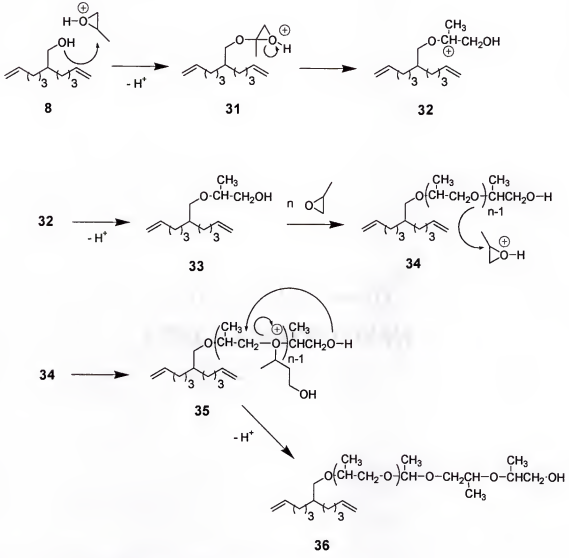

Figure 3-12. "Back-biting" of polyether polymerizations.

ADMET Polymerization of PPO Macromonomers

The ADMET polymerization of macromonomer (**36**) using Grubbs' first generation ruthenium benzylidene catalyst and was monitored by NMR techniques. However, as

indicated by the ^{1}H NMR spectrum (Figure 3-14), complete conversion of α,ω-dienes (**28**) to internal olefins (**37**) did not occur. The unsuccessful partial polymerization is attributed to the steric bulk and high degree of functionality associated with the PPO chains which hinder catalyst activity.

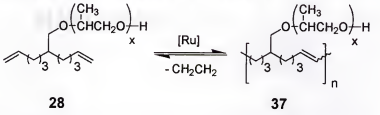

28 **37**

Figure 3-13. Polypropylene oxide macromonomer ADMET polymerization.

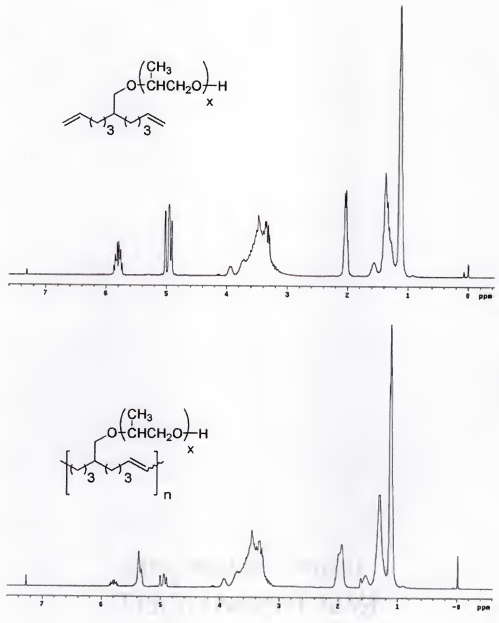

Figure 3-14. ^{1}H NMR of ADMET polymerization for PPO macromonomer (**28**).

Anionic Polymerizations

Anionic polymerizations take place in monomers with electron withdrawing groups in ligands or rings (Elias 1997). These are composed of styrene and its derivatives,

aldehydes, ketones, isocyanates, oxiranes, thiiranes, carboxy anhydrides, lactams, and lactones (Figure 3-15). Anionic polymerizations are often difficult to achieve because growing anionic chains react readily with proton donating impurities such as water which terminate the polymerization. Therfore, these types of polymerizations require strictly "dry" solvent conditions and expensive initiators.

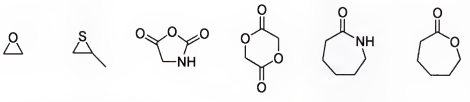

Figure 3-15. Anionic ring opening monomers.

Anionic Initiation

Bronsted or Lewis bases are used to initiate anionic polymerizations by alkali metals, alkoxides, amines, phosphines, or sodium naphthalene. As previously indicated, these polymerizations occur in solvent, and the initiators can dissociate spontaneously under the proper conditions into the initiating anions. The dissociation then results in polymerization with little or no thermal activation energy. Initiator ions may also be generated from monomers through electron transfers. This is the case when naphthalene reacts with sodium metal in THF to form a naphthalide radical anion (**38**). This dissolves in THF which allows the radical anions to become stabilized through THF interactions (Figure 3-16). Upon polymerization with styrene (**39**), the electrons of the naphthalene anion are transferred to styrene molecules in an equilibrium reaction resulting in styryl radical anions (**40**) that dimerize to distyryl dianions (**41**). These distyryl dianions then begin polymerizing by sequential monomer addition.

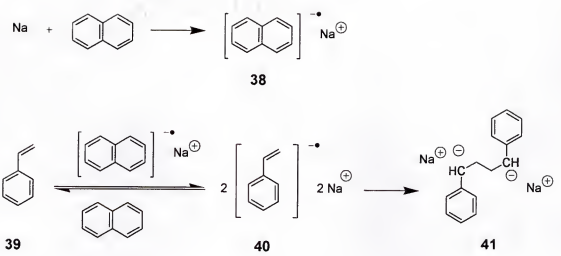

Figure 3-16. Sodium naphthalide radical anion initiation.

Anionic Propagation and Termination

After initiation, the macroanion continues to propagate in a "living" manner until all of the initial monomers are polymerized. Ideal "living" polymerizations do not exhibit termination or chain transfer reactions. Anionic polymerizations rarely endure spontaneous terminations and are deliberately terminated by added agents such as water or alcohols. This method chain ends the polymerization with a proton and protects against depolymerization and other unwanted side reactions. Chain transfer reactions also terminate macroanions, but a new anion produces and initiates a new polymer chain. Termination reactions allow the introduction of a desired functional end group.

Ethylene Oxide Anionic Ring Opening Polymerization

Long chain polyether grafts were introduced into the α,ω-diene monomer through the inititation of ethylene oxide polymerization with a primary alcohol functional group (Figure 3-17) resulting in macromonomer (**42**). The alcohol was deprotonated with potassium naphthalide to initiate the "living" anionic conditions. Ethylene oxide was polymerized via ring opening through quantitative amounts to obtain the desired chain

length. It should be noted that the use of ethylene oxide requires extreme caution. It is a highly volatile gas at room temperature which is explosive and poisonous.

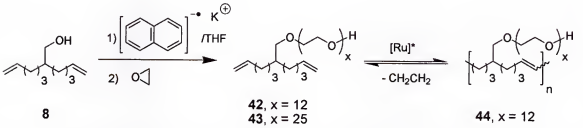

Figure 3-17. Macromonomer synthesis and polymerization of extended polyether chains.

To aid in the structural characterization of these large monomers (**43**), MALDI-TOF analysis was used to gather precise molecular weight data. MALDI-TOF provides absolute molecular mass information which is difficult to measure by commonly employed analytical methods such as NMR and GPC. Data for macromonomer (**43**) was collected (Figure 3-18) and has led to further clarification of the polymerization mechanism. The macromonomer was analyzed with *all-trans*-retinoic acid as the matrix and copper (II) chloride as the cationization agent in THF. The number of ethylene oxide repeat units was determined to be 25, a value in agreement with that obtained from ^{1}H NMR. In addition, the polydispersity of the ethylene oxide graft was calculated to be 1.06 from this spectrum. An expanded view of the MALDI-TOF spectrum of macromonomer (**43**) illustrates cationization by Cu^+, Na^+, and K^+. It was noted that Na^+ and K^+ were adventitious ions arising from the solvent. Consequently, the number- and weight-average molecular weights were corrected for the shift due to this occurrence. MALDI-TOF analysis demonstrates the precision by which these macromonomers were prepared. Very narrow polydispersities were evident, and graft lengths were able to be chosen at will.

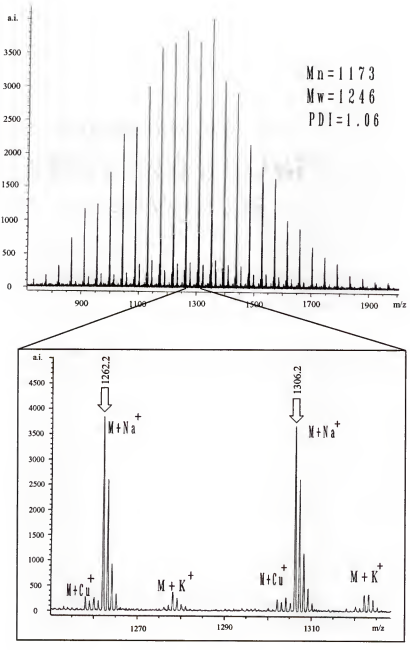

Figure 3-18. MALDI-TOF analysis of polyether macromonomer (**43**).

The precise nature of graft placement in this chemistry suggests the possibilty of producing "perfect" polyether comb polymers that mimic the behavior of crown ethers. There is possible evidence of this behavior is displayed in Figure 3-19. The spectrum portrays the cationization agent, copper (II) iodide, interacting in a specific dimerizing

coordination manner with the macromonomer (**43**). Inspection of the spectrum reveals a second set of peaks at approximately 2500 m/z which uneviquocally illustrates the coordination of polyether grafts with the copper ion. Each polyether-based graft operates independently of one another in the copolymer as long as there is sufficient spacing between graft sites; thus, the potential for specific ion bonding exists. Since each grafted polyether chain exhibits lower entropy than its analogous free chain, complexation regarding the crown ether is enhanced. Consequently, these graft copolymers portray the potential to become useful in specific metal complexation without exhibiting the toxic effects related to true crown ether structures.

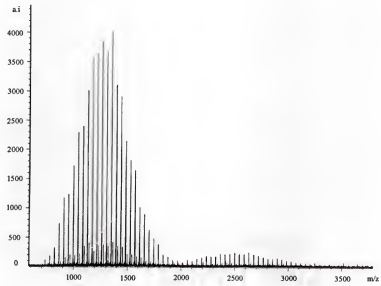

Figure 3-19. MALDI-TOF of the copper coordination process.

ADMET Polymerization of PEG Macromonomers

While the short chain polyether grafts polymerize by ADMET techniques with relative ease, the longer chain graft comonomers have proven to be more difficult. The ^{1}H NMR spectra (Figure 3-20) indicates the degree of polymerization is lower for significantly

extended grafts (**43a**, Table 3-1). Apparently, the long chain PEG units self-organize to complex the catalyst, thereby decreasing the extent of polycondensation. With the advent of Grubbs' seceond generation benzylidene ruthenium catalyst, a higher molecular weight copolymer can be achieved (**43b**, Table 3-1). The polymerization can be performed at higher temperatures with the second generation catalyst (Lehman and Wagener 2002), increasing entropy of macromonomer. This allows the terminal olefins enough disorder to become unhindered from the PEG chains and react with the metal carbene of the catalyst.

Table 3-1. Molecular weight data of PEO based graft copolymers.

	M_n (GPC)	PDI (GPC)	M_n (NMR)	n
12	15000	2.23	NA	60
37	2000	2.61	1700	5
44a	5500	1.45	3500	8
44b	12000	2.15	7100	17

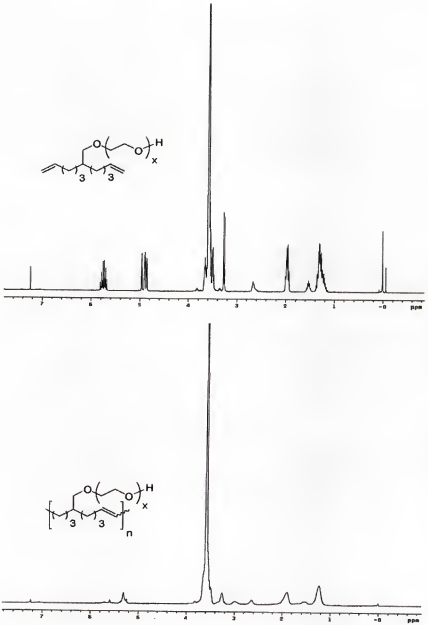

Figure 3-20. ^{1}H NMR of polyether macromonomer (**42**) conversion to copolymer (**44**).

Discrepancy between ^{1}H NMR and GPC results can be attributed to the fact that GPC is not an absolute method but rather it's based upon relative polystyrene standards which do not behave in the same manner as the graft copolymers in solution.

Summary

This chapter discussed the synthesis and characterization of the first succesful "perfect comb" graft copolymers using ADMET techniques combined with conventional "living" polymer chemistry techniques. Factors such as steric bulk and monomer functionality were determined to play a crucial role in the extent of polymerization. The monomer synthesis is straightforward and the resulting graft materials show promise in a number of applications such as metal complexation as "crown ether mimics" and drug delivery systems.

CHAPTER 4
COPOLYMERS BY ATOM TRANSFER RADICAL POLYMERIZATIONS

Free radical polymerizations have become one of most important commercial processes leading to high molecular weight polymers and account for approximately one half of all the worlds polymers (Patten and Matyjaszewski 1998). This process is significantly useful because it allows for a large diversity of monomers to be polymerized and copolymerized under simple experimental conditions (Moad and Solomon 1995). However, a consequence of these types of polymerizations is that they lack molecular weight control and often lead to ill-defined structures with broad polydispersities. In 1995, a new class of controlled / "living" radical polymerizations was reported independently by two separate groups of Sawamoto (Kato et al. 1995) and Matyjaszewski (Wang and Matyjaszewski 1995). By definition, "living" polymerizations are chain-growth polymerizations that proceed in the absence of irreversible chain transfer and termination (Szwarc 1956, Matyjaszewski 1993). Since that time, controlled / "living" radical polymerizations have developed into one of the most significant methods in organic polymer chemistry. The ability to produce well-defined, high molecular weight polymers with low polydispersities from a broad variety of monomers applies well to commercialization and allows for continued research in academia.

Controlled / "Living" Radical Polymerizations

Catalysis Mechanism

The use of transition metal catalysts has been known for a long time in radical polymerizations. However, these catalyst systems often lead to ill-defined structures. It

was not until the development of a copper complex that controlled / "living" radical polymerizations, or more specifically, atom transfer radical polymerizations (ATRP), produced defined structures by radical methods (Bellus 1985). ATRP uses a reversible metal catalyzed atom transfer mechanism to generate the propagating radical which contrast it from conventional controlled / "living" radical methods that utilize photochemical or thermal homolytic cleavage.

The ATRP cycle proceeds in a manner that regenerates the propagating radical. During polymerization (Figure 4-1), the metal complex (**1**) undergoes a one-electron oxidation by abstraction of the halogen atom from the starting compound (**3**). This reaction generates an organic radical (**4**) and copper (II) complex (**2**). The substituents on the organic halide facilitate the reaction by stabilizing the radical. The radical then adds to an unsaturated group (**5**) in an inter- or intra-molecular fashion resulting in a terminal propagating terminal radical (**6**). Re-abstraction of the halogen atom from the copper (II) complex then occurs to reform the original copper (I) complex terminating the radical resulting in the product (**6**). The initial cycle is known as Atom Transfer Radical Addition (ATRA). ATRP occurs upon continuation of the atom transfer equilibrium that regenerates (**6**) and deactivates the propagating radicals from the initiator or a polymer chain end. The role of the initiator (**3**) during the polymerization cycle is to determine the number of dormant chains and to provide the structure of the initiating end of the polymer chain. After activation of a dormant chain, more than one monomer can add to the chain and the number of additions that occur before termination determines the degree of polymerizattion. Even though the persistent radical effect will minimize the

total number of chains terminated by coupling or disproportionation, irreversible chain terminations must still be accounted for (Patten and Matyjaszewski 1999).

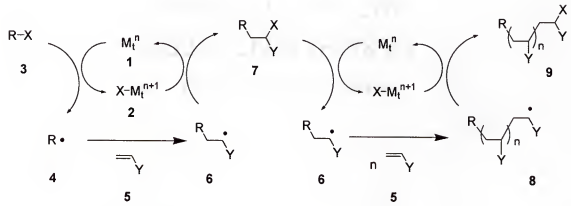

Figure 4-1. ATRP mechanism.

ATRP is a radical polymerization system which is a reversible process based upon the activation and deactivation of propagating radicals. The activation rate constant for the an inner sphere electron transfer reaction between the alkyl halide (**3**) and transition metal (**1**) to form a radical (**4**) and metal halide (**2**) is $k_a = 10^{-1\pm1}$ $M^{-1}s^{-1}$. Deactivation occurs when the propagating radical (**4**) reacts with the metal halide (**2**) to reform the alkyl halide (**3**) thus lowering the oxidation state of the transition metal. The rate constant is for deactivation is typically $k_d = 10^{7\pm1}$ $M^{-1}s^{-1}$. The equilibrium constant, $K = k_a/k_d$, is dependent upon variables of the polymerization system such as solvent, temperature, ligand choice, monomer, halogen, and metal. The deactivation process is fast and it's responsible for obtaining good control of molecular weight and narrow polydispersities.

Determining whether the nature of the radical polymerization was a free radical or mediated by a metal center was not straightforward as described by Matyjaszewski (1999). There is no single factor that can accurately determine the reaction mechanism;

rather a combination of several criteria determine the nature of the propagating species. This includes chemoselectivity (reactivity ratios for copolymerizations), stereoselectivity (tacticity of the resulting polymer), regioselectivity (structure of end groups), and elucidation of termination (coupling/disproportionation). In addition, the development of reverse ATRP has supports the nature of the radical mechanism. In this system (Figure 4-2), the transition metal catalyst is initially in a high oxidation state, ex. $Cu(II)Cl_2/L$. In the presence of a conventional free radical initiator such as AIBN, the radical reacts with the metal halide to form the alkyl halide thus lowering the oxidation state of the metal. After almost all of the initiator and metal halide have been consumed, the controlled / "living" radical polymerization begins.

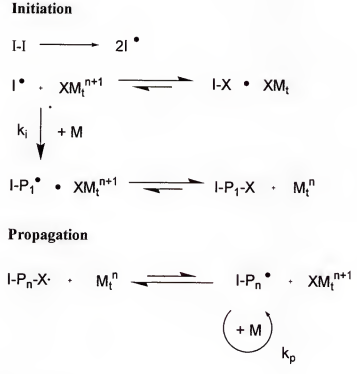

Figure 4-2. Reverse ATRP.

It was reported that the homogenous ATRP of styrene, acrylate, and methacrylate allows for excellent degrees of polymerization up to DP ~ 100 and polydispersities, M_w/M_n, as low as 1.04 to 1.05 (Patten and Matyjaszewski 1996). ATRP minimizes side reactions such as termination, elimination of HX from the chain end, and oxidation / reduction of the radicals to the corresponding cation / anion (Matyjaszewski 1997). Unlike chain polymerizations of conventional radical conditions, controlled / "living" polymerizations are first order kinetics with respect to monomer concentration (Figure 4-3) and are typically in close agreement with the calculated values based upon $([M]_o - [M]_t)/[In]_o$. The same conversions were also reported for polymerizations conducted in solvents such as diphenyl ether, *p*-dimethoxybenzene, or benzophenone. As expected, conversion rates were slower than bulk polymerizations as expected due to the lower concentration of the initiating system.

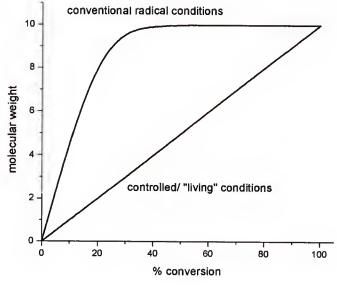

Figure 4-3. Comparison of conventional vs. controlled radical polymerization kinetics.

ATPR Catalyst Requirements

In order for ATRP catalysts to perform efficiently, there are several requirements that must be fulfilled. An ATRP catalyst should be selective, efficient, and be able to dynamically change between two oxidation states, robust and inexpensive (Matyjaszewski 2000).

Ideally, ATRP catalysts should be involved in the reversible atom transfer but not in any other reactions. This goal can be accomplished through optimization of the reaction conditions through adjustment of the steric and electronic properties of the complex by the appropriate ligands. The goal is to accomplish inner sphere electron transfer and avoid reactions such as β-hydrogen abstraction or an outer sphere electron transfer process which lead to the oxidation and formation of organometallic species.

The equilibrium constant is one of the most important parameters of the catalyst since it defines the proportion of radicals generated by the transition metal complex. Essentially a higher equilibrium constant is more favorablw since the same amount of radicals can be formed with a lower concentration of the transition metal complex. However, if the equilibrium constant is too high, an excessive amount of radicals may lead to an exceedingly high contribution of radical termination and loss of control. Most systems operate with equilibrium constants in the range of $10^{-9} < K < 10^{-6}$.

An ATRP catalyst exists in two oxidation states where the activator is M_t^n/L in the lower oxidation state and $X\text{-}M_t^{n+1}/L$ is the deactivator in the higher oxidation state. These catalysts are easily oxidized to the higher oxidation state. The equilibrium constant between the two states defines the overall amount of radicals and polymerization rate. The number of monomer units added during each activation step is determined by

the rate ratios of propagation to termination. Only a few monomer units should add during each step for a controlled ATRP process. Thus, the deactivation process may be as fast as diffusion control.

Finally, the robustness and stability of ATRP catalysts is critical for the catalyst to retain its original activity after each cycle. If these requirements are not achieved during the polymerizataion process, the catalyst may become complexed by the monomer or polymer which may lead to the displacement of the original ligand from the coordination sphere and reduce catalytic activity. The released ligand may then become involved in other unwanted side reactions.

Controlled Architecture by ATRP

ATRP conditions allow for control over the structure through the initiator and active end group. Therefore, polymer chains have the ability to be end-functionalized and copolymerized with other monomers. This control offered by ATRP furthers the development of new polymeric materials with novel topologies (linear, combs, stars, networks and dendrimers) and varying compositions (blocks, random, alternating, gradients, grafts) which grant the placement of different functionality in the macromolecule (Patten and Matyjaszewski 1998).

Several approaches have been used to prepare graft copolymers using ATRP, and all of them share the common theme of utilizing initiating groups or polymerization methods to prepare the two segments. The first method involves the polymerization of monomers possessing substituents capable of initiating ATRP. Two different approaches were reported in the preparation of the macroinitiator (Beers et al. 1998). The first involved a conventional radical homopolymerization of 2-(2-bromopropionyloxy)-ethyl acetate (**10**, BPEA) using AIBN as the initiator (Figure 4-4).

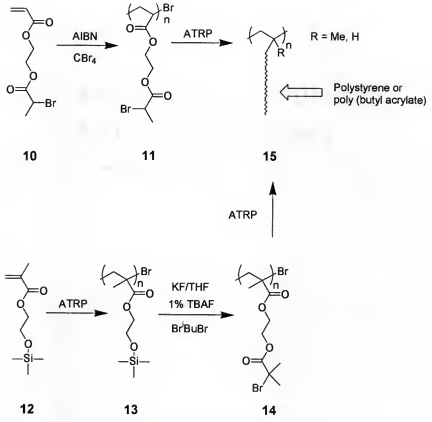

Figure 4-4. Macroinitiator approach to ATRP graft copolymers.

However, using AIBN as an initiator resulted in a broad molecular weight distribution. Despite the highly controlled polymerization of the side chains, the resulting graft copolymer (**11**) yielded a broad polydispersity. Therefore, the development of a well-defined macroinitiator was achieved by polymerizing a trimethylsilyl protected 2-hydroxyethyl methacrylate (**12**, HEMA-TMS) by ATRP methods. The macroinitiator (**13**) was then deprotected to yield a different macroinitiator, poly-(2-(2-bromoisobutyryloxy)ethyl methacrylate) (**14**, pBIEM). This method resulted in a well controlled, molecular weight and narrow polydispersity macroinitator that was suitable for ATRP of styrene and butyl acrylate. These copolymers with pendant α-bromoester

groups led to graft copolymers composed of a soft polymer backbone segment and hard graft polymer segment to yield a thermoplastic elastomer (**15**).

Another approach that was utilized in the preparation of graft copolymers through "living" radical methods was the "grafting through" technique which involved the copolymerization of macromonomers made from other living or conventional techniques (Figure 4-5).

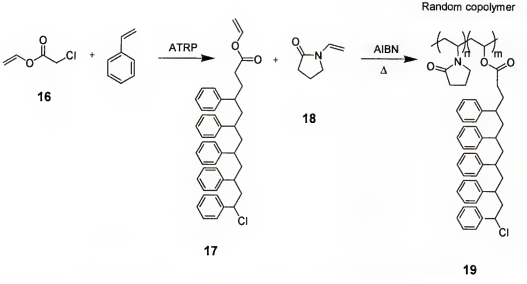

Figure 4-5. Grafting through approach of ATRP generated macromonomers.

Polystyrene macromonomers (**17**) were prepared by ATRP methods with a vinyl chloroacetate initiator (**16**) and then copolymerized with N-vinyl pyrrolidine (**18**) to form high molecular weight graft copolymers (**19**) (Matyjaszewski et al. 1998). This method was developed because the ATRP technique can be applied to a larger range of monomers than other "living" methods. Thus, this would expand the number of monomers available for making macromonomers and an increase in thier versatility. Due to the opposing hydrophilicities of the copolymerization segments, these copolymers will

dissolve in DMF but only swell in hydrocarbons or water. In water, the copolymers form hydrogels with 80-95% equilibrium water content.

Metathesis and ATRP

Macromolecular architectures have also been developed through a combination of ATRP and metathesis polymerizations. The integration of ring-opening metathesis (ROMP) with ATRP has aided in the development of novel block copolymers. This development was first reported by Grubbs (Bielwaski et al. 2000a) to synthesize ABA triblock copolymers of poly (styrene)-b-poly (butadiene)-b-poly (styrene). Telechelic butadienes were end-capped with the appropriate chain transfer agent which served as ATRP initiators, and then polymerized with styrene. These materials were found to be useful for commercial applications such as thermoplastic elastomers. The synthetic route proved to be an effective bifunctional macroinitiator for ATRP. In addition to building triblock copolymer structures, Grubbs extended the development of ATRP and ROMP by synthesizing a single catalyst capable of a simultaneous dual polymerizations (Bielwaski et al. 2000b). This ruthenium complex (**20**) was the first example of a complete ATRP system containing both the transition metal mediator with a radical initiator combined in a single complex. The ability to prepare block copolymers (**23**) was demonstrated by performing ROMP and ATRP in a "one pot" synthesis with the ruthenium-based catalyst (**20**) in the presence of 1,5-cyclooctadiene and methyl methacrylate (Figure 4-6). Nearly monodisperse copolymers were obtained and living conditions were indicated by a linear relationship between monomer conversion and polymer molecular weight was observed.

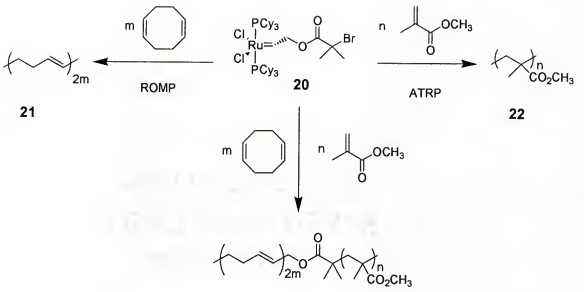

Figure 4-6. Tandem ROMP and ATRP catalysis of AB block copolymers.

ADMET and ATRP

The combination of ATRP and metathesis methods was further explored by integrating ADMET to development graft copolymers. Design of the macromolecular architecture was accomplished via two different synthetic pathways to acquire the same product. As previously discussed, both macromonomer and macroinitiator methods have their advantages and disadvantages (Figure 4-7). The macroinitiator route proceeds with polycondensation of the symmetrical α,ω-diene (**24**), achieving a higher polymer backbone molecular weight. Without the presence of stericly hindered grafts attached to the polyolefin backbone, the catalyst is capable of approaching the metathesizing terminal olefins. The monomer is still a liquid at this point, and the metathesis polymerization can be easily performed in bulk conditions under high vacuum. Upon following metathesis with atom transfer radical polymerization, the stoichiometry of the system must be exact in order to initiate all functional sites simultaneously and there is no

guarantee that all sites will initiate. Typical polymer characterization methods such as ^{1}H and ^{13}C NMR and GPC are unable to confirm regioregularity along the polymer backbone. Thus, it cannot be confirmed that graft regularity occurs along the polymer backbone with 100% certainty. On the other hand, if the macromonomer approach is employed, then the monomer (**26**) will contain the graft within the α,ω-diene functionality, and the molecular weight of the resulting macromonomer can be predetermined through "living" polymerization conditions prior to metathesis. Not only will the polymer backbone be regioregular with respect to graft placement, but full characterization of the macromonomer will exist prior to ADMET. Most macromonomers of this nature are solids, and the polycondensation must be performed with solvent conditions. In addition, the sterics of the grafted chains interfere with catalyst approach to the diene functionality thereby hindering the rate of the metathesis polymerization.

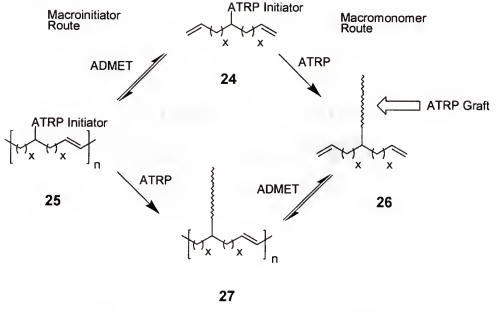

Figure 4-7. ADMET/ATRP synthetic approaches toward graft copolymers.

Thermoplastic Elastomers

Several unique properties have been developed based upon the combination of different materials in an ordered fashion. These advancements have been possible due to achievments in "living" polymerization techniques that allow for precise architecture control. For example, in the past block copolymers composed of crystalline and amorphous domains have been studied as thermoplastic elastomers (Ryan et al. 1995, Park et al. 2000, Zhu et al. 2000). Thermoplastic elastomers exhibit a rubber-like behavior without chemical cross-linking that are softened upon heating and reshaped in processing (Schollengerg et al. 1958). The glass transition (T_g) or melt transition temperature (T_m) of the "hard" segment must be above the use temperature of the material while remaining low enough for melt processing. The "soft" polymer segment should be amorphous or semicrystalline with a low T_g (Fetters 1973). The chains of the amorphous phase need to be able to slip past each other, allowing the material to elongate. Meanwhile, the hard domains act as physical anchors preventing the soft chains from stretching beyond the point of recovery. Finally, the relative proportions of the two segments is important and must be considered for achieving elastic behavior. It was with these concepts that the exploration of combining "hard" crystalline segments with "soft" semicrystalline segments in a graft copolymer architecture was undertaken.

ADMET readily synthesizes polyolefins, which are considered "soft" segments. By grafting "hard" polymers, such as polystyrene or poly(methyl methacrylate) to the polyolefin backbone, the materials will be unlike either homopolymer or random copolymer. The physical behaviors of these graft copolymers will be left for a later discussion in Chapter 5. The remainder of this chapter will discuss the preparation of these materials.

Macroinitiator Synthesis

The ATRP initiator was synthesized from a primary alcohol (**3.8** or **3.9**) prepared in the same manner discussed in Chapter 3. It was necessary to functionalize the alcohol with a radical stabilizing tertiary bromide by a coupling reaction with 1,3-dicyclohexylcarbodiimide (DCC) and 2-bromo-2-methyl propionic acid (Figure 4-8). It was also possible to utilize 1-(3-dimethylaminopropyl)-3-ethylcarbodiimide (EDC) or 1,3-diisopropylcarbodiimide (DIC) couplings and obtain similar results. Purification was accomplished by simply passing over silica gel, and the structure was confirmed through ^{1}H and ^{13}C NMR, elemental analysis and mass spectroscopy (**29**).

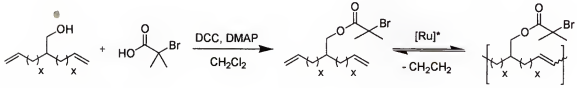

3.8, x = 3
3.9, x = 9

28, x = 3
29, x = 9

30, x = 3
31, x = 9

Figure 4-8. ATRP macroinitiator synthesis and polymerization.

Metathesis of the ATRP initiator (**29**) was performed in neat conditions under high vacuum. This polymerization is fairly novel, and the reaction was monitored by ^{1}H NMR for the conversion of the terminal olefin peaks at 4.98 and 5.81 ppm to an internal olefin peak at 5.37 ppm which indicated a fairly high degree of polymerization (Figure 4-9). This result is typical of ADMET conditions and in agreement with data obtained from GPC. Typical molecular weights of these reactions are in the range of M_n = 17,000 to 33,800 with a polydispersity range of 1.96 to 2.05.

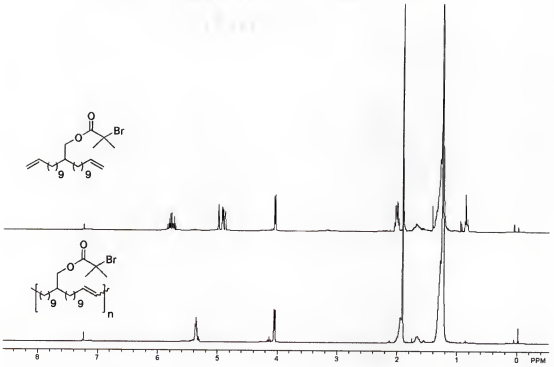

Figure 4-9. ADMET polymerization of ATRP initiator (**30**).

Macroinitiator Polymerization

After successful metathesis polycondensation, the polyolefin macroinitiator (**29**) was prepared for grafting by removing the ruthenium benzylidene catalyst with tris (hydroxy) phosphine (TPA) isopropanol solution donated from Materia (Pasadena, CA). Following precipitation from methanol, an approximation of the initiator sites along the polyolefin backbone was determined through GPC measurements in order to calculate the proper initiator:catalyst:monomer ratio of the "living" polymerization. These calculations are critical for attaining simultaneous initiation of the polymerization so that each graft will be the same length. ATRP was performed with styrene as the monomer and copper bromide with 2,2'-bipyridine as the catalyst system. GPC indicated a monomodal peak

and a molecular weight increase of M_n = 17,000 to M_n = 20,0000 and only a slight increase in the polydispersity from 2.05 to 2.32, confirming successful grafting of polystyrene to the polyolefin backbone (Figure 4-10).

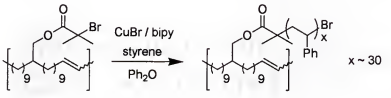

31 **32**

Figure 4-10. ATRP polymerization of the polyolefin macroinitiator.

Each repeat unit of polystyrene correlates to a molecular weight of 104 g/mol and the data acquired from the GPC correlates to a chain length of 30 repeat units for each repeat unit of the polyolefin backbone (**32**). The abundance of polystyrene in the NMR spectrum also indicates a successful addition of the polystyrene chains to the polymer backbone. However, due an excessive amount of polystyrene in the macromolecule, it is difficult to differentiate between the two types of polymer chains. The instrument cannot lock onto both polymer chains since the sample is composed of two fundamentally different polymers. Even at increased concentration levels, elongated relaxation times and extended transitions, the polystyrene component dominates the system and it is still difficult to acquire a conclusive spectrum. A ^{1}H NMR spectrum of commercial polystyrene displays the broad peaks associated with the sample and how the chemical shifts are in the same regions as the methylene peaks of the polyethylene based backbone (Figure 4-11). Unfortunately, as previously discussed, these characterization techniques may indicate a successful reaction, but they are unable to ensure that all functional sites were initiated during ATRP.

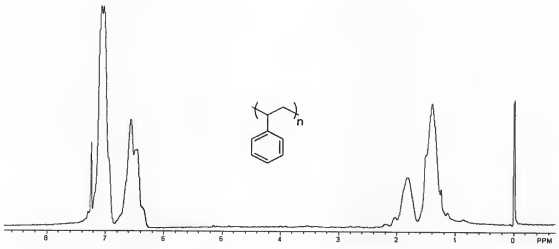

Figure 4-11. ^{1}H NMR of commercial polystyrene.

Macromonomer Synthesis and Polymerization

The macromonomer method was employed to improve upon structure control and characterization of these materials. The polystyrene grafts were attached to the symmetrical diene with controlled / "living" techniques prior to ADMET as discussed in Chapter 3. Since the molecular weight of the ATRP initiator (**29**) is precisely known, the initiator:catalyst:monomer ratio is more accurate than the macroinitiator method. In turn, a more precise graft length will result. Various graft lengths of polystyrene with 15 (**33**) and 30 repeat units (**34**) were prepared by ATRP methods from the functionalized tertiary bromide (Figure 4-12).

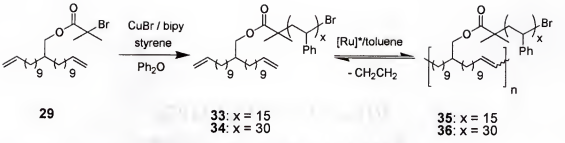

Figure 4-12. ATRP macromonomer synthesis and polymerization.

The copper catalyst was removed and polystyrene macromonomers (**33** and **34**) were precipitated into MeOH. Several characterization techniques were used to confirm graft length. However, as with the macroinitiator samples, the abundance of the polystyrene chain floods the α,ω-diene functionality and other methylenes in both ^{1}H and ^{13}C NMR, and the resolution becomes lost in the baseline. It was only in the spectrum of the shorter polystyrene chains (**35**) that the terminal olefin peaks at 4.99 and 5.81 pm were distinguishable from the baseline (Figure 4-13). Once the polystyrene chain was extended to 30 repeat units (**36**), the terminal olefins were no longer be observed.

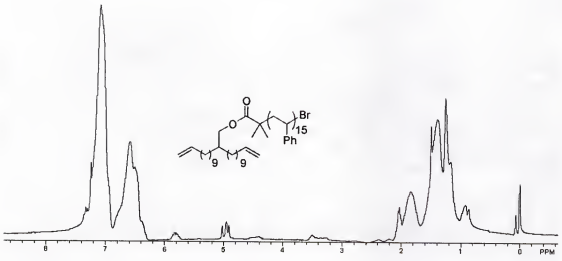

Figure 4-13. ^{1}H NMR of polystyrene macromonomer (**33**).

Since precise molecular weight characterization is often difficult to acquire by NMR and other types of analysis, the macromonomers were analyzed by matrix-assisted laser desorption/ionization (MALDI-TOF). This method of analysis was found helpful in obtaining absolute molecular weight information with molecules synthesized by ATRP methods (Nonaka et al. 2001). The polystyrene macromonomer samples were prepared with copper bromide as the ionizing agent in a dithranol matrix and dissolved in THF. The data obtained from MALDI-TOF analysis for **33** (Figure 4-15) and **34** (Figure 4-16) were in close agreement with the calculated values indicating the proper controlled / "living" conditions were present during the polymerization. In addition, the MALDI-TOF values were in close agreement with data obtained from GPC measurements (Table

4-1). The high correlation can be attributed to the fact that polystyrene standards were used during calibration of the instrument, which allowed for similar behavior of macromonomers in the elution solvent.

Table 4-1. Molecular weight data of polystyrene macromonomers and graft copolymers.

	M_n (GPC)	PDI (GPC)	M_n (MALDI)	PDI (MALDI)
33	2300	1.15	2241	1.16
34	3000	1.18	2837	1.26
35	10400	4.85		
36	6300	4.79		

During MALDI analysis, two sets of peaks were observed with a difference of 14 mass units higher and 91 mass units below. The mass of 91 accounts for the cleaved diene functionality (**39**) from the polystyrene chain (**37**). The samples underwent a rearrangement and cleavage during proton ionization. This rearrangement is commonly known as the McLafferty rearrangement and has been well documented (Silverstein et al. 1991). This rearrangement is a migration of hydrogen atoms in molecules that contain heteroatoms as a result of intramolecular atomic rearrangement during fragmentation (Figure 4-14). Therefore, the second set of peaks observed is attributed to this phenomenon.

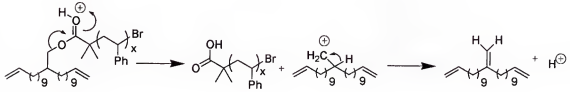

33 or **34** **37** **38** **39**

Figure 4-14. McLafferty rearrangement.

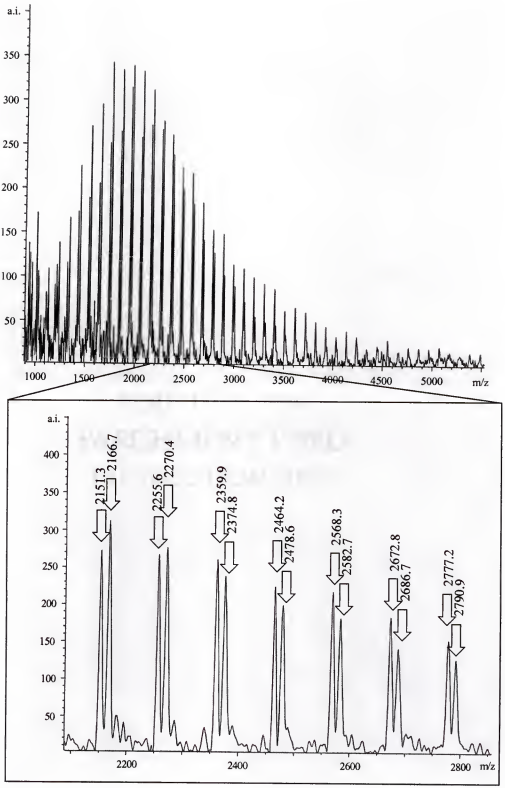

Figure 4-15. MALDI-TOF of polystyrene macromonomer **33**.

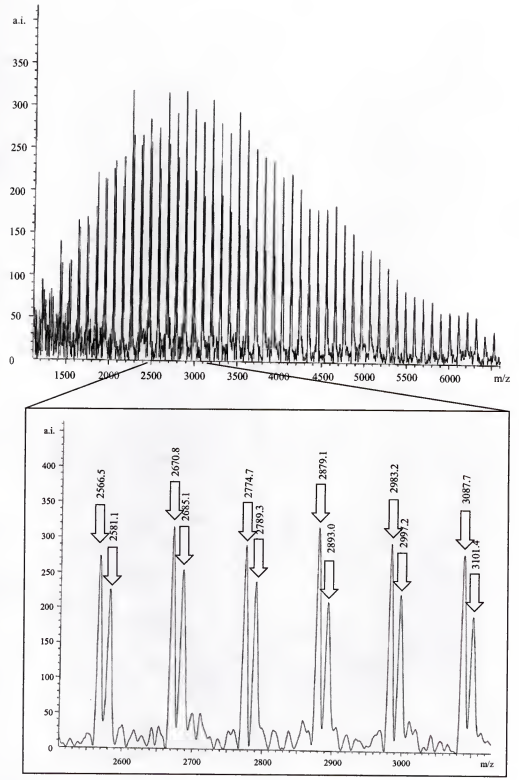

Figure 4-16. MALDI-TOF of polystyrene macromonomer **34**.

The solid macromonomers were dried and prepared for ADMET polymerization upon full characterization. However, typical bulk metathesis conditions were unable to be performed since the monomers were solids. The polycondensation reactions required solvent conditions in order to allow the reaction to proceed. This added another dimension to the polymerization, and it was determined that a correlation existed between both the polarity of the solvent and macromonomer. Multiple attempts were made with several different solvents such as toluene, hexanes, chloroform, methylene chloride, and tetrahydrofuran. Due to the nonpolar nature of the polystyrene macromonomers the metathesis polymerizations would have to be performed in a nonpolar solvent. Toluene was determined to be the best solvent for a successful polymerization. In addition, steric bulk caused by the polystyrene chains along the polyolefin backbone eventually hindered the approach of the catalyst to the olefin functionality. To attain high molecular weight polymers, extended reaction times of 10 days and heated systems from 65 to 75°C were required. Absence of the terminal olefins and the conversion to internal olefin in the ^{1}H NMR indicated a successful metathesis polymerization (Figure 4-17). As previously discussed, the presence of two different polymers provides difficulty in fully characterizing these materials by NMR techniques. The shifts of the $\underline{CH_2}$ protons pendant to the backbone become lost in the baseline, and it becomes difficult to observe the internal olefin peaks at 5.39 ppm. However, GPC measurements did indicate a significant increase in molecular weight from macromonomer to graft copolymer with an increase in polydispersity which is characteristic of ADMET conditions. Also, a significant increase in the polydispersity was a result of these polymerizations conducted

in solution (Table 4-1). These results can be attributed to the alkylidene's ability to locate the functionality of the terminal olefin in solution.

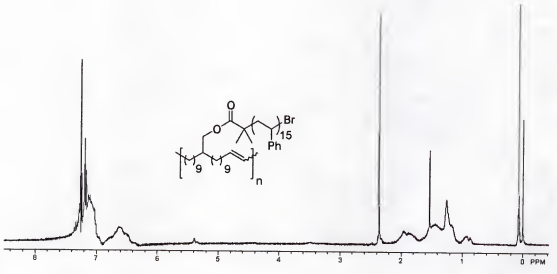

Figure 4-17. ^{1}H NMR of ADMET polyolefin-g-polystyrene (**35**).

Summary

By preparing different chain lengths of polystyrene graft copolymers, ATRP has shown to be capable of preparing well-defined macromolecules in combination with metathesis polymerizations. Specifically, ATRP has been found to be useful in synthesizing macromonomers that can be fully characterized prior to polycondensation resulting in absolute certainty of the graft nature, length, and placement in the final copolymer structure. These are significant improvements upon the macroinitiator method.

CHAPTER 5
GRAFT COPOLYMER THERMAL INVESTIGATIONS

Thermal analysis, also know as thermal spectroscopy, measures the heat-energy change that occurs in a substance as a function of temperature. It is possible to measure a physical transition or chemical reaction that is accompanied by a heat-energy change since most changes in the physical state and chemical reactions are accompanied by a change in enthalpy.

Phase Separation

By integrating two polymers of differentiating properties into one macromolecule via covalent bonds, a propensity for phase separation exists. The differing chains have a predisposition to separate from each other with minimal interactions, yet the covalent bonds prevent a complete phase separation. This tendency to separate with molecular connectivity is known as microphase separation in copolymer systems. Although the microphase separation phenomenon had been established by the Strasbourgh School (Skoulious et al. 1960, Sadron 1963), it was not understood until Holden and Milkovich (1964) discovered its use in block copolymers for useful properties. As observed with graft copolymers, microphase separation may lead to unique properties. At times, copolymer systems develop microscopic domains of each parent homopolymer where thermal characteristics, as well as other properties, may be retained in the copolymer (Holden 1973, Cowie 1973).

The extent and nature of phase separation is influenced by several factors such as temperature, pressure, miscibility of the homopolymers, and the lengths and relative

volumes of the two components (Holden 1973). The influence of relative volumes with respect to phase separation has been investigated in great detail (Molau 1971, Basset 1981, Woodward 1994). General morphologies exist in different forms consisting of a minor component within a matrix of the dominating component or continuous phase (Figure 5-12). By increasing the amount of the minor component, different forms occur within the matrix to minimize the interfacial interactions between the two domains. The minor component exists in an embedded spherical form as the major domain is in large excess. This is then driven to cylindrical domains as the volume of the minor component increases. As the two components approach equal proportions, a layered, lamellae morphology exists.

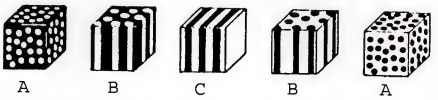

Figure 5-1. Primary modes of phase separation in a two-component copolymer system: a) spherical; b) cylindrical (rods); c) lamellae. Image was reproduced from the Ph.D. Dissertaton of Zuluaga (1993).

Differential thermal analysis offers significant insight into phase separated materials. The greater the degree of phase separation within the material, the more distinct the thermal transitions corresponding to the homopolymers will be retained.

Analysis of Phase Separation

Several analytical methods have proven useful when studying phase seperated materials. For example, gel permeation chromatography (GPC), small angle X-ray (SAXS) and electron microscopy all provide insight to the nature of the domains. GPC

provides information about molecular weight and the distribution of the copolymer matrix. If a fraction of low molecular weight homopolymer species is present in a copolymer system, it is often indicated by a bimodal peak (Noshay and McGrath 1977). In addition to information about molecular weight distributions, data about the size and shape of the domains can be acquired through SAXS. This method can determine the size of the domains for copolymers in which one, or both, of the components crystallize. Domains can be also be examined for cases where morphology is highly ordered (Nielson 1991, Gedde 1995). Finally, microphase seperated materials can be studied by electron microscopy. This technique perhaps offers the most information about these systems because an image of the morphlogies is actually produced (Gedde 1995). Surface structures are examined by scanning electron microscopy (SEM) and information about the bulk structure is provided by transition electron microscopy (TEM). Electron microscopy typically requires selective staining of one component in order to invoke a contrast in the electron densities between the two blocks.

In addition to the previous methods, differential scanning calorimetry (DSC) has proven to be very useful in the investigation of microphase separation. Experimentally, it is a direct measurement in which a sample is heated with respect to an inert reference material at a uniform rate, measuring the difference in temperature between the two samples. The degree of phase mixing is indicated by the deviation from a thermal transition, such as a glass transition temperature (T_g) or melt transition temperature (T_m). The presence of separate T_g or T_m values coinciding with those of the homopolymers is an indication of phase separation.

It is the intent to discuss the thermal characteristics of the graft copolymers prepared in the previous chapters. By combining polymers of different compositions in such an ordered fashion, the resulting thermograms should behave in a different manner compared to the original homopolymer or random copolymer. In addition, the combination of fundamentally different "hard" polystyrene segments and "soft" polyolefin segments may lead to microphase separation due to the influence of the final equilibrium of the ordered states. Very few studies on microphase separation have been performed on graft copolymers since it is typically required that one of the segments be crystalline in order for microphase separation to occur, as with $(A\text{-}B)_n$ type block copolymers (Gibson et al. 1982). However, graft copolymers can have multiphase morphologies depending upon their structure and homogeneity (Evans et al. 1975, Tsai et al. 1986).

Thermal Behaviors of Polymer Systems

Thermal transitions are used to characterize polymeric materials and their domains through glass and/or melt transition temperatures. The glass transition temperature (T_g) is the temperature at which amorphous domains translate to the glassy state and become brittle, stiff, and rigid in character. It is the point at which long-range motion of the polymer is stopped. Long-range motion, also known as segmental motion, is the movement of a segment of a polymer chain by the concerted rotation of bonds at the end of the segments. On the other hand, the melt transition temperature (T_m) is the temperature at which the crystalline domains of the polymer melt. This temperature describes the fashion at which packing occurs and how the ordered lattice arranges upon crystallization. It is important to study these transitions because of the insight they offer regarding structural and property relationships for a given macrostructure.

Polyoctenamer Thermal Behavior

The primary focus of the preceding chapters was on linear polymerizations through metathesis condensation affording a regular polyolefin. All of the graft copolymers were synthesized with this method; thus, it is necessary to examine a non-branched polyolefin.

The polymerization of 1,9-decadiene under bulk ADMET conditions with Grubbs' first generation benzylidene catalyst affords a polyoctenamer in which the melt transition temperature occurs with an onset at 59°C and peaks at 67°C (Figure 5-2). Upon hydrogenation of the polymer backbone, the melt transition temperature increases to 134°C due to the removal of the unsaturated bond. The increase of the melt transition is attributed to the polymer chain packing in a more ordered fashion. Removal of the kinks in the polyolefin backbone allow for a higher degree of arrangement.

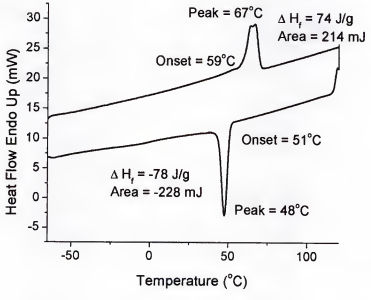

Figure 5-2 Polyoctenamaer synthesized from Grubbs' first generation catalyst.

With the advent of Grubbs' second generation benzylidene catalyst, the polymerization of 1,9-decadiene under the same bulk conditions afforded a linear polyolefin with quite different results (Figure 5-3). After three continous thermal scans, the melt transition occured with an onset at 35°C and a bimodal peak at 43°C. The decrease in the melt transition temperature was most likely be attributed to an isomerization process that occured during the metathesis polymerization. As with the first generation catalyst, hydrogenation of the unsaturated polymer backbone increased the melt transition temperature to 134°C.

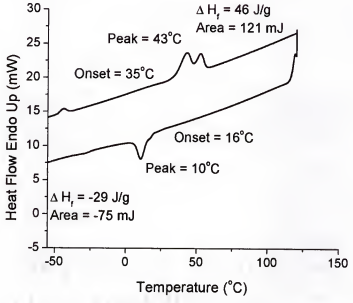

Figure 5-3. Polyoctenamer synthesized from Grubbs' second generation catalyst.

ADMET polymerization of 1,9-decadiene in solvent conditions with toluene resulted in a thermogram similar to bulk conditions. Again, a bimodal melt transition peak was observed with an onset of 32°C and a peak at 42°C (Figure 5-4). Yet under these reaction conditions, the bimodal distribution is not as pronounced. There is still an indication of

the isomerization process by the bimodal distribution and a decrease in the melt transition temperature when compared to the thermogram of the first generation catalyst.

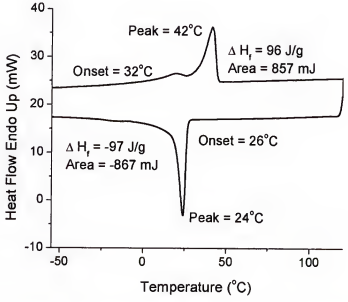

Figure 5-4. Polyoctenamer synthesized from Grubbs' second generation catalyst in solution conditions.

Poly(ethylene oxide) Thermal Behavior

Poly(ethylene oxide) exhibited typical semicrystalline thermal behavior by exemplifying an amorphous region with a glass transition temperature at –41°C and a crystalline region with a melt transition temperature at 63°C (Figure 5-5). Upon cooling, the material recrystallized at 31°C in a quantitative manner as indicated by the change in enthalpy.

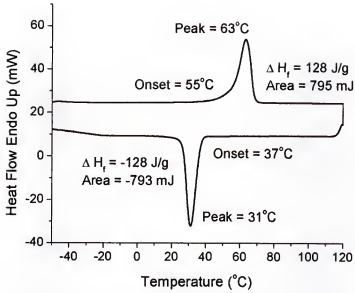

Figure 5-5. Poly(ethylene oxide) standard with M_n = 100,000.

Poly(ethylene oxide) macromonomer thermal analysis

Poly(ethylene oxide) macromonomers exhibited vastly different thermal properties compared to the poly(ethylene oxide) standards. Upon heating, a glass transition occurred with an onset at –85°C. In addition, a cold crystallization exotherm was indicated by the peak occurring at –61°C followed by a rather broad melt endotherm initiated at –7°C (Figure 5-6). This is a rather interesting observation because cold crystallizations are known to occur in polymers such as polydimethylsiloxsanes and quenched poly(ethylene terephthalate).

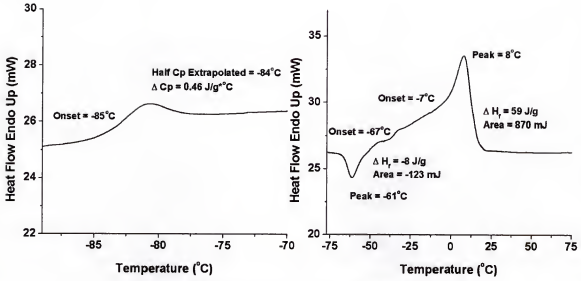

Figure 5-6. Poly(ethylene oxide) macromonomer.

The thermal behavior of quenched poly(ethylene terephthalate) (PET) is a known process, and the crystallization has been, and continues to be, investigated (Bikales 1971, Jog 1995, Zhao et al. 2002). Similar to PET, the poly(ethylene oxide) chains of the macromonomer attain a sufficient amount of mobility after the glass transition temperature. This mobility is what allows for the formation of the crystallites in the region of the cold crystallization. Upon continued heating, the crystallites are undergo long range melting as indicated by the broad exotherm. The PET thermogram indicates that the material is crystallized from the melt and contributes to long range ordering, similar to the pattern observed with the poly(ethylene oxide) macromonomers.

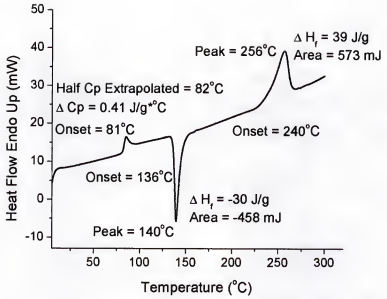

Figure 5-7. Thermal analysis of poly(ethylene terephthalate) standard.

Poly(ethylene oxide) graft copolymer thermal analysis

Upon metathesis of the of poly(ethylene oxide) macromonomer, the unannealed samples of the long chain comb copolymers displayed interesting thermal behavior (Figure 5-8). This was apparently due to its well-ordered system. An initial endotherm occurred at –52°C with an onset at –54°C was the result of melting the well-defined, tethered poly(oxyethylene) grafts. After the initial melt of the grafts took place, an immediate exotherm occured at –44°C as a result of cold crystallization of the unsaturated polyolefin backbone. As heating continued, the newly formed polyolefin crystals melted at 0°C with an onset occurring at –12°C. A glass transition temperature was also observed with an onset at –68°C. This was most likely a reflection of the polyether amorphous phase of the copolymer.

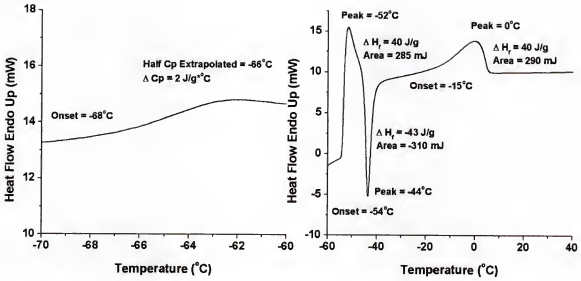

Figure 5-8. Poly(ethylene oxide)-g-olefin copolymer.

Short polyether graft copolymers

Thermal analysis of the short polyether (methoxy ethoxy methyl) grafts along the polyolefin backbone resulted in a completely amorphous material in which a glass transition temperature had an onset of –90°C. The short polyether chains were not long enough to crystallize, as in the extended poly(ethylene oxide) graft copolymers. The polymer morphology was composed of tethered grafts which hindered the lamellae from chain folding in an ordered fashion, preventing any crystallization.

Polystyrene Thermal Behavior

The thermal behavior of polystyrene is simplistic and straight forward due to its amorphous character (Figure 5-9). The glass transition temperature of polystyrene is a

direct consequence of steric factors such as chain flexibility and tacticity. A high glass transition was obtained since large pendant groups are attached to the chain restricting its internal rotation and impeding crystallization. However, crystallization can be induced through regular stereochemical arrangements such as isotactic and syndiotactic polystyrene. As a consequence of crystallization in the polymer, the glass transition is also lowered (Cowie 1973).

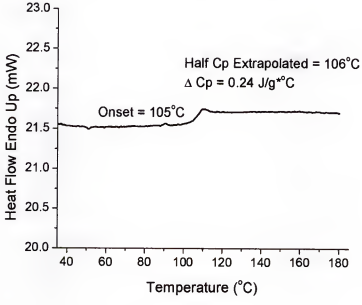

Figure 5-9. Atactic polystyrene standard.

Polystyrene macromonomer thermal analysis

The synthesis of relatively short amorphous polystyrene chains by "living" ATRP methods to functionalize ADMET precursors resulted in glass transition temperature that were greatly decreased as a result of the α,ω-diene functionalized chain ends. As the polystyrene chain was shortened, a decrease in the glass transition temperature was demonstrated by a polystyrene chain with 30 repeat units resulted in a T_g of 35°C and a

polystyrene chain of 15 repeat units resulted in a T_g of 20°C (Figure 5-10). It is thought that translation of a polymer chain proceeds by a means of segmental jumps involving short units, usually consisting of 15 to 30 chain atoms. Complete movement of the chain is affected by the surrounding chains. Considerable entanglement exists, and any other motion will be retarded by other chains. The polymer molecule may drag along several other chains, and the energy dissipation is a combination of friction between the chain and those entangled with the neighboring chains as they slip past each other (Cowie 1973). Thus more energy is required to invoke long chain segmental motion of the glass transition temperature.

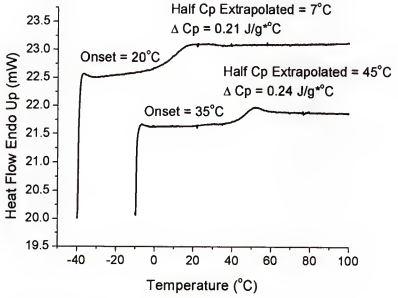

Figure 5-10. Polystyrene macromonomers. (Top) Thermal trace of short chain polystyrene macromonomer. (Bottom) Thermal trace of extended chain polystyrene macromonomer.

Polystyrene graft copolymer thermal analysis

After metathesis of the polystyrene macromonomers, the glass transition temperatures for both short and extended polystyrene graft copolymers chain increased to an onset of 60°C (Figure 5-11).

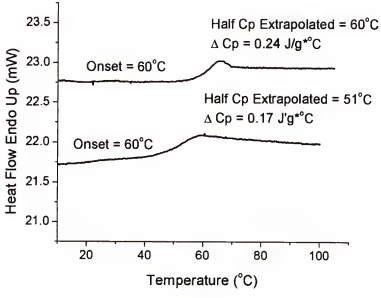

Figure 5-11. Polyolefin-g-polystyrene. (Top) Thermal trace of short polystyrene graft copolymer. (Bottom) Thermal trace of extended polystyrene graft copolymers.

The increase in glass transition was attributed to the morphological composition of the polystyrene and polyoctenamer backbone. Obviously, the length of the side chain no longer effects thermal properties, but rather architectural constraints continue to influence the segmental motion in a manner which is different from either of the homopolymers or random copolymers (Richards 1992, Privalko and Novikov 1995). As discussed earlier, the extent of polymerization also influences the resulting glass transition temperature. In this situation, it is likely that since the shorter polystyrene chains had a greater degree of

polymerization compared to the extended polystyrene chains, a similar copolymer molecular composition resulted since both glass transitions are approximately equivalent.

Random Copolymer Thermal Behavior Studies

To induce a greater degree of microphase separation between the domains of the polystyrene grafts and polyolefin backbone, a copolymer model study was performed in which the short and extended polystyrene branched macromonomers of the previous section were polymerized with 1,9-decadiene (Figure 5-12). This model study allowed for a thorough investigation of the effects of both glass and melt transition temperatures.

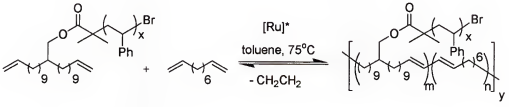

1 **2** **3-10**

a, x =15
b, x = 30

a, x =15
b, x = 30

Figure 5-12. Copolymerization scheme of polystyrene macromonomers and 1,9-decadiene.

The metathesis polycondensation reactions were performed in toluene at an elevated temperature of 75°C under a slight argon purge for a period of 10 days. Integration of the α-methylene compared to the methylidene peak of the internal olefin by NMR indicated an increase in the polyolefin character as the molar concentration of 1,9-decadiene was increased. In addition to NMR, an increase in M_n by GPC also indicated a conversion of the internal olefin. The calculated molar ratios were in agreement to experimental results according to ^1H NMR and GPC (Table 5-1). However, as previously discussed with homopolymerization of the macromonomers, polydispersity of these copolymerizations

were rather broad due to solvent conditions. In addition, GPC peaks of the extended polystyrene chains (**8-10**) were bimodal in character, indicating that block segments of homopolymers formed during ADMET polymerization indicated that the reactivity of the α,ω-dienes with extended polystyrene macromonomers (**1b**) was decreased as a result of the steric bulk of the side chains. This behavior was not observed in GPC analysis of the shorter polystyrene chains (**1a**), signifying a statistical random copolymer.

Table 5-1. Molecular weight data of copolymerization.

	x	mol% 1	mol% 2	% **2** (NMR)	M_n (GPC)	PDI(GPC)
3	a	100	0	0	10400	4.85
4	a	75	25	50	13800	3.59
5	a	50	50	80	7500	1.95
6	a	25	75	90	11600	2.87
7	b	100	0	0	6300	4.79
8	b	75	25	40	13600	4.34
9	b	50	50	75	8000	3.95
10	b	25	75	90	9400	4.37

GPC results were acquired in THF at 35°C with polystyrene standards.

There was no indication of phase separation upon thermal analysis of the short chain polystyrene graft copolymers (**4-6**). In fact, the copolymers maintained an amorphous state and never crystallized (Figure 5-13). However, a correlation between molar concentration and glass transition temperature was observed in which increasing the polyolefin character increased T_g. As with the homopolymerization of the macromonomers (**3** and **7**), the properties of the homopolymers morphed together resulting in unique properties.

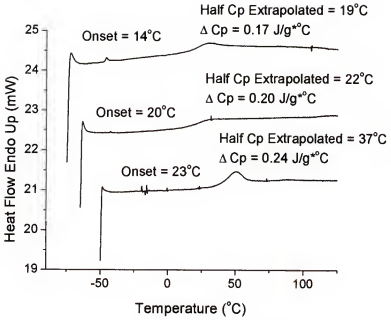

Figure 5-13. (Top) Thermal trace of short polystyrene chain (**4**). (Middle) Thermal trace of short polystyrene chain (**5**). (Bottom) Thermal trace of short polystyrene chain (**6**).

In addition to the short chain polystyrene macromonomers, thermal investigations of the extended polystyrene chains copolymers was also conducted. Microphase separation of the hard and soft domains was not observed in materials with low concentrations of polyolefin character. A copolymer with 40 mol% polyoctenamer character (**8**) yielded an amorphous material with a glass transition temperature onset of 44°C (Figure 5-14).

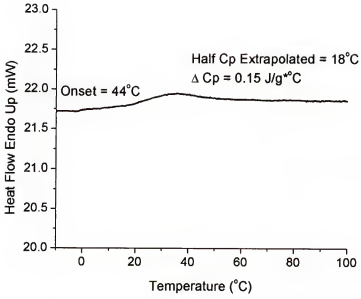

Figure 5-14. Glass transition temperature of 40 mol% polyoctenamer character copolymer (**8**).

The thermograms for extended polystyrene chain copolymers consisting of 75% mol (**9**) and 90% mol (**10**) polyoctenamer character were scanned from -75°C to 150°C (Figure 5-15). Analysis of the thermal scans indicated a broad melt transition peak for the 75 mol% with an onset of 23°C and a peak at 39°C. After increasing the the polyoctenamer composition to 90 mol%, the melt transition maintained its peak of 39°C while becoming significantly more pronounced with an onset of 33°C. The crystalline behavior observed in these thermograms was a direct result of increasing the polyolefin character. These results indicated phase separation of the polystyrene chains from the polyoctenamer backbone. There are two factors of the synthesis which account for this behavior. First, by decreasing the concentration of the graft along the polymer backbone, the polyolefin is unhindered to fold in an organized manner and crystallize. Second, by performing the copolymerization with sterically bulky, extended polystyrene chains, the formation of segmented graft copolymers with homopolymer runs did not permit the

amorphous polystyrene chains to interfere with the crystallization of the backbone. No other melt transitions were observed for the graft network due to of the amorphous polystyrene character.

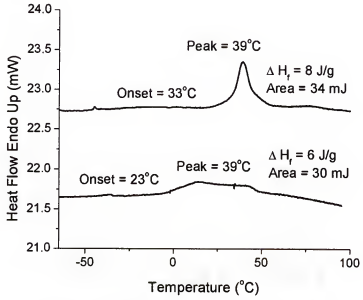

Figure 5-15. Crystallization of graft copolymers **9** (bottom) and **10** (top).

Summary

Thermal analysis investigations provides helpful insight into the behavior of complex macromolecular architectures. Several observations about the complex graft copolymer architectual design were illustrated by the combination of fundamentally different segments. In particular, the comparison of hydrophilic grafts combined with hydrophobic backbones, and the combination of "hard" polystyrene grafts with "soft" polyolefin backbone segments were investigated because of their differentiating physical properties. It was determined that the thermal outcome of these copolymer systems were fundamentally different from either of the homopolymers or random copolymer.

LIST OF REFERENCES

Battaerd, H.A.J.; Tregear, G.W. *Graft Copolymers*; Wiley & Sons: New York, 1967.

Bassett, D.C. *Principles of Polymer Morphology*; Cambridge University Press: New York, 1981.

Bednarek, M.; Kubisa, P.; Penzcek, S. *Macromolecules* **2001**, *34*, 5112.

Bellus, D. *Pure Appl. Chem.* **1985**, *57*, 1827.

Beers, K.L.; Gaynor, S.G.; Matyjaszewski, K.; Sheiko, S.S.; Moller, M. *Macromolecules* **1998**, *31*, 9413.

Biedron, T.; Brzezinska, K.; Kubisa, P.; Penczek, S. *Polym. Int.* **1995**, *36*, 73.

Bielawski, C.W.; Louie, J.; Grubbs, R.H. *J. Am. Chem. Soc.* **2000b**, *122*, 12872.

Bielawski, C.W.; Morita, T. Grubbs, R.H. *Macromolecules* **2000a**, *33*, 678.

Brzezinska, K.; Szymanski, R.; Kubisa, P.; Penczek, S. *Makromol. Chem., Rapid Comm.* **1986**, *7*, 1.

Brzezinska, K.R.; Wagener, K.B. Burns, G.T. *J. Poly. Sci. A: Polym. Chem.* **1999**, *37*, 849.

Burchard, W. *Advances in Polymer Science*, Springer, New York, vol 143, **1999**.

Church, A.C.; Smith, J.A.; Pawlow, J.H.; Wagener, K.B. Non-Traditional Step-Growth Polymerization-ADMET. In *Synthesis Methods in Step-Growth Polymers*; Long, T.E.; Rodgers, M., Ed.; Wiley & Sons: New York, Ch. 9, in press.

Cossy, J.; BouzBouz, S.; Hoveyda, A.H. *J. Organomet. Chem.* **2001**, *634* (2), 215.

Cowie, J.M.G. *Polymers: Chemistry and Physics of Modern Materials*; Billing and Sons Ltd: Worcester, 1973.

Crabtree, R.H. *The Organometallic Chemistry of the Transition Metals*, 2nd edition; Wiley and Sons: New York, 1994.

Davidson, T.A.; Wagener, K.B. Acyclic Diene Metathesis (ADMET) Polymerization. In *Synthesis of Polymers*; Schluter, A.D., Ed.; Materials Science and Technology Series; Wiley-VCH: Wienheim, 1999, p.105.

Edgecomb, B.D.; Stein, J.A.; Frechet, J.M.J.; Xu, Z.H.; Kramer, E.J. *Macromolecules* **1998**, *31*, 1292.

Elias, H.G. *An Introduction to Polymer Science*; VCH: New York, 1997.

Elsenbroich, C.; Salzer, A. *Organometallics: A Concise Introduction*; VCH: New York, 1992.

Evans, D.C.; George, M.H.; Barrie, J.A. *Polymer* **1975**, *16*, 690.

Fetters, L.J. Synthesis of Elastomeric Block Copolymers by Anionic Polymerization. In *Block and Graft Copolymerization*, Vol. 1, Ceresa, R.J., Ed.; Wiley and Sons, New York, 1973.

Fischer, J.P. *Angew. Chem., Int. Ed. Engl.* **1973**, *12*, 428.

Gedde, U. *Polymer Physics*, Chapman & Hall, New York, 1995.

Gibson, P.E.; Vallance, M.A.; Cooper, S.L. *Development in Block Copolymers*; Goodman, I.,Ed.; Applied Science: London, 1982.

Gomez, F.J.; Wagener, K.B. *Macromol. Chem. Phys.* **1998**, *199*, 1581.

Grubbs, R.H.; Chang, S. *Tetrahedron* **1998**, *54*, 4413.

Grubbs, R.B.; Hawker, C.J.; Dao, J.; Frechet, J.M.J. *Angew. Chem. Int. Ed. Engl.* **1997b**, *36*, 270.

Grubbs R.H.; Marsella, M.J.; Maynard, H.D. *Angew. Chem. Int. Ed. Engl.* **1997a**, *36*, 1101.

Hallden, A.; Ohlsson, B.; Wesslen, B. J. *Appl. Polym. Sci.* **2000**, *78*, 2416.

Harris, J.M. *PEG Chemistry: Biotechnical and Biomedical Applications*; Plenueum Press: New York, 1992.

Herrmann, W.A.; Kratzer, R.M.; Fischer, R.W. *Angew. Chem. Int. Engl. Ed.*, **1997**, *36,* 2652.

Herrison, J.L.; Chauvin, Y. *Makromol. Chem.* **1970**, 141.

Hoffman, A.S.; Bacskai, R. *Copolymerization*; Ham, G.E., Ed.; Interscience: New York, 1964.

Holden, G. Properties and Applications of Elastomeric Block Copolymers. In *Block and Graft Copolymerization*, Ceresa, R.J., Ed.; Wiley & Sons: New York, 1973, vol 1.

Holden, G.; Milkovich, R. U.S. patenet 3,265,765 **1964** (to shell).

Huang, J.; Stevens, E.D.; Nolan, S.P.; Petersen, J.L. *J. Am. Chem. Soc.*, **1999**, *121*, 2674.

Ivin, K.J.; Mol, J.C. *Olefin Metathesis and Metathesis Polymerization*; Academic Press: San Diego, 1997.

Jerome, R. *Macromol Chem. Phys.* **1999**, *200,* 156.

Jog, J.P. *J. Macromol. Sci., Rev. Macromol. Chem. Phys.* **1995**, *C53*, 531.

Kato, M.; Kamigaito, M.; Sawwamoto, M.; Higashimura, T. *Macromolecules* **1995**, *28*, 1721.

Ke, B *Characterization of Polymers*; Nikales, N.M., Ed.; Wiley and Sons: New York, 1971.

Kennedy, J.P.; Charles, J.J.; Davidson, D.L. *Recent Advances in Polymer Blends, Grafts and Blocks*; Sperling, L.H., Ed.; Plenum: New York, 1974.

Kobatake, S.; Harwood, H.J.; Quirk, R.P.; Priddy, D.B. *Macromolecules* **1998**, *31*, 1292.

Lehman, S.E.; Wagener, K.B. *Macromolecules* **2002**, *35*, 48.

Matyjaszewski, K. *Macromolecules* **1993**, *26*, 1787.

Matyjaszweski, K. *Tetrahedron* **1997**, *53*, 15321.

Matyjaszewski, K. *Education in Advanced Chemistry*; Marcinec, B., Ed.; Wydawnicto Poznanskie: Poznan, 1999, vol 6.

Matyjaszewski, K. *Polym. Prepr. (Am. Chem. Soc., Div. Polym. Chem.)* **2000**, *41*(1), 411.

Matyjaszweski, K.; Beers, K.L.; Kern, A.; Gaynor, S.G. *J. Polym. Sci., Polym. Chem.* **1998**, *36*, 823.

Mercerryes, D.; Dubois, Ph.; Jerome, R.; Hendrick, J.L. *Macromol. Chem. Phys.* **1999**, *200*, 156.

Moad, G.; Solomon, D. *The Chemistry of Free-Radical Polymerization*; Pergamon: Oxford, 1995.

Molau, G. E. Ed. *Collodial & Morphological Behavior of Block and Graft Copolymers*; Plenum: New York, 1971.

Morton, M.; Fetters, L.J. *Macromol. Rev.* **1967**, *2*, 71.

Nakagawa, Y.; Matyjaszweski, K. *Polym. Prepr. (Am. Chem. Soc., Div. Polym. Chem.)* **1996**, *37*(2), 270.

Neilson, L.E. *Modern Methods of Polymer Characterization*, Wiley, New York, 1991.

Nonaka, H.; Ouchi, M.; Kamigaito, M.; Sawamoto, M. *Macromolecules* **2001**, *34*, 2083.

Noshay, A.; McGrath, J.E. *Block Copolymers*; Academic Press Inc.: New York, 1977.

Nguyen, S.T., Grubbs R.H.; Ziller, J.W. *J. Am. Chem. Soc.*, **1993**, *115*, 9858.

Nubel, P.O.; Yokelson, H.B.; Lutman, C.A. *Macromolecules* **1995**, *27*, 7000.

O'Donnell, P.M.; Brzezinska, K.; Powell, D.; Wagener, K.B. *Macromolecules* **2001**, *34*, 6845.

Odian, G. *Principals of Polymerization*, 3rd edition; Wiley Interscience: New York, 1991.

Park, C.; De Rosa, C.; Fetters, L.J.; Thomas, E.L.; *Macromolecules* **2000**, *33*, 7931.

Patten, T.E.; Matyjaszewski, K. *Adv. Mater.* **1998**, *10*, 901.

Patten, T.E.; Matyjaszewski, K. *Acc. Chem. Res.* **1999**, *32*, 895.

Patten, T.E.; Xia, J.; Abernathy, T.; Matyjaszewski, K. *Science* **1996**, *272*, 866.

Penzcek, S.; Kubisa, P. *Ring-Opening Polymerization*; Brunelle, D.J., Ed.; Hasner Publishers: Munich, 1993, p.13.

Privalko, V.P.; Novikov, V.V. *The Science of Heterogeneous Polymers: Structure and Thermophysical Properties*; Wiley and Sons: New York, 1995.

Richards, R.W. Block Copolymers. *Multicomponent Polymer Systems*; Miles, I.S.; Rostami, S., Ed.; Longman and Scientific & Technical: New York, 1992.

Roberts, M.J.; Harris, J.M. *Pharm. Sci.* **1998**, *87*, 1440.

Ryan, A.J.; Hamley, I.W.; Bras, W.; Bates, F.S. *Macromolecules* **1995**, *28*, 3860.

Sadron, C. *Angew. Chem. Int. Ed. Engl.* **1963**, *2*, 248.

Schaverien C.J.; Dewan, J.C.; Schrock, R.R. *J. Am. Chem. Soc.*, **1986**, *108*, 2771.

Scholl, M.; Ding, S.; Lee, C.W.; Grubbs, R.H. *Org. Lett.*, **1999**, *1*, 953.

Schollengerg, C.S.; Scott, H.; Moore, G.R. *Rubber World* **1958**, *137*, 549.

Schrock, R.R. *Acc. Chem. Res.* **1990**, *23*, 158.

Schrock, R.R. Ring Opening Polymerization. *Ring Opening Polymerization*; Bruneile, D.J., Ed.; Hanser: Munich, 1993, p.129.

Schwab, P.E.; Grubbs, R.H..; Ziller, J.W.; *J. Am. Chem. Soc.*, **1996**, *118*, 100.

Schwendeman, J.; Wagener, K.B *Polym. Prepr. (Am. Chem. Soc. Div. Polym. Chem.)* **2002a**, *43* (1), 280.

Schwendeman, J.; Wagener, K.B *Polym. Prepr. (Am. Chem. Soc. Div. Polym. Chem.)* **2002b**, *43* (1), 282.

Shinoda, H.; Miller, P.J.; Matyjaszewski, K. *Macromolecules* **2001**, *34*, 3186.

Silverstein, R.M.; Bassler, G.C.; Morrill, T.C. *Spectroscopic Identification of Organic Compounds*, 5th edition; Wiley and Sons, Inc.: New York, 1991.

Skoulious, A.; Finaz, G.; Parrod, G. *Comp. Rend.* **1960**, *251*, 739.

Smith, J.A.; Brzezinska, K.R.; Valenti, D.J.; Wagener, K.B. *Macromolecules* **2000**, *33*, 3781.

Stannett, V.J. *Macromol. Sci., Chem.* **1977**, *4*, 1177.

Szwarc, M. *Nature* **1956**, *178*, 1168.

Szwarc, M. *Carbanions, Living Polymers and Electron Transfer Processes*; Interscience: New York, 1968.

Tindall, D.; Pawlow, J.H.; Wagener, K.B. Recent Advances in ADMET Chemistry. *Alkene Metathesis in Organic Synthesis*; Furstner, A., Ed.; Springer-Verlag: Berlin, 1998, p.183.

Tindall, D; Wagener, K.B.; Brzezinska, K.R. *Polym. Prepr. (Am. Chem. Soc. Div. Polym. Chem.)* **1999**, *218* (2), 413.

Tobolsky, A.V., *Structure and Properties of Polymerization*; Wiley & Sons: New York, 1960.

Trnka, T.M.; Grubbs, R.H. *Acc. Chem. Res.*, **2001**, *34*, 18.

Tsai, C.H.Y.; Thomas, E.L.; McNight, W.J.; Schneider, N.S. *Polymer* **1986**, *27*, 659.

Valenti, D.J.; Wagener, K.B. *Macromolecules* **1998**, *31*, 2764.

Wagener, K.B.; Boncella, J.M.; Nel, J.G. *Macromolecules*, **1991**, *24*, 2694.

Wagener, K.B.; Boncella, J.M.; Nel, J.G.; Duttweiler, R.P.; Hilmeyer, M.A. *Makromol. Chem.*, **1990**, *191*, 365.

Wagener, K.B.; Brzezinska, K.; Anderson, J.D.; Dilocker, S. *J. Poly. Sci. A: Polym. Chem.* **1997b**, *35*, 3441.

Wagener, K.B.; Brzezinska, K.; Anderson, J.D.; Younkin, T.R.; Steppe, K.; DeBoer, W. *Macromolecules*, **1997a**, *30*, 7363.

Wang, J.S.; Matyjaszewski, K. *J. Am. Chem. Soc.* **1995**, *117*, 5614.

Watson, M.D.; Wagener, K.B. *Macromolecules* **2000a**, *33*, 3196.

Watson, M.D.; Wagener, K.B. *Macromolecules* **2000b**, *33*, 8963.

Weskamp, T.; Schattenmann, W.C.; Spieglar, M.; Herrmann, W.A. *Angew. Chem. Int. Engl. Ed.*, **1998**, *37,* 2490.

Weskamp, T.; Kohl, F.J.; Hieringer, W.; Gleich, D.; Herrmann, W.A. *Angew. Chem. Int. Engl. Ed.*, **1999**, *38,* 2416.

Woodward, A.E. *Understanding Polymer Morphology*; Hanser-Garden: New York, 1994.

Wright, D. *Current Organic Chemistry* **1999**, *3*, 211.

Zhao, X.; Harris, J.M. *Pharm. Sci.* **1998**, *87*, 1450.

Zhao, J.; Yang, J.; Song, R.; Linghu, X.; Fan, Q. *Europ. Polym. J.* **2002**, *38*, 645.

Zhu, L.; Cheng, S.Z.D.; Calhoun, B.H.; Ge, Q.; Quirk, R.P.; Thomas, E.L.; Hsiao, B.S.; Yeh, F.; Lotz, B. *J. Am. Chem. Soc.* **2000**, *122*, 5957.

Zuluaga, F. Chemistry of Poly(Ether-Ester) and Siloxane Based Thermoplatic Elastomers. Ph.D. Dissertation, The University of Florida, 1993.

BIOGRAPHICAL SKETCH

Patrick M. O'Donnell was born April 18, 1974, to John and Barbara O'Donnell in Iowa City, Iowa. He only lived in Iowa for only a short time as his father completed his Ph.D. in medicinal chemistry. Patrick's family then moved to Yonkers, New York, for a year and eventually settled in Morgantown, WV, in 1976. It was here where Patrick was raised with strong family values and graduated from Morgantown High School in May 1992. Patrick then started college that fall at West Virginia University and declared chemistry as his major. After studying natural product synthetic methods with Dr. Kay Brummond, Patrick decided to attend graduate school and received his B.A. degree in May 1996. He remained at WVU for a postbacalaureate until May 1997 and then moved to Gainesville, FL, in August as a graduate student at the University of Florida under the direction of Dr. Kenneth Wagener in the division of organic polymer synthesis. Patrick received his Ph.D. in August 2002 and accepted a postdoctoral position at the University of Massachusetts, Amherst, with Dr. E. Bryan Coughlin in the field of polymer science and engineering to develop fire resistant polymers.

I certify that I have read this study and that in my opinion it conforms to acceptable standards of scholarly presentation and is fully adequate, in scope and quality, as a dissertation for the degree of Doctor of Philosophy.

Kenneth B. Wagener, Chairman
George B. Butler Professor of Polymer Chemistry

I certify that I have read this study and that in my opinion it conforms to acceptable standards of scholarly presentation and is fully adequate, in scope and quality, as a dissertation for the degree of Doctor of Philosophy.

John R. Reynolds, Co-Chairman
Professor of Chemistry

I certify that I have read this study and that in my opinion it conforms to acceptable standards of scholarly presentation and is fully adequate, in scope and quality, as a dissertation for the degree of Doctor of Philosophy.

Eric Enholm
Professor of Chemistry

I certify that I have read this study and that in my opinion it conforms to acceptable standards of scholarly presentation and is fully adequate, in scope and quality, as a dissertation for the degree of Doctor of Philosophy.

Jon D. Stewart
Associate Professor of Chemistry

I certify that I have read this study and that in my opinion it conforms to acceptable standards of scholarly presentation and is fully adequate, in scope and quality, as a dissertation for the degree of Doctor of Philosophy.

Christopher Batich
Professor of Materials Science and Engineering

This dissertation was submitted to the Department of Chemistry in the College of Liberal Arts and Sciences and to the Graduate School and was accepted as partial fulfillment of the requirements for the degree of Doctor of Philosophy.

August 2002

_____

Dean, Graduate School